Research Report

No. 82-3

REALIZABLE ARM FILTERS IN I AND Q RECEIVERS FOR MSK-TYPE CONTINUOUS PHASE MODULATIONS

PREPARED FOR
THE DEPARTMENT OF COMMUNICATIONS
UNDER DSS CONTRACT No. OSU81-00246

BY

D.J. VAISEY P.J. MCLANE

MARCH 1982

Queen's University at Kingston
Department of Electrical Engineering

Checked 11/83

REALIZABLE ARM FILTERS IN I AND Q RECEIVERS FOR MSK-TYPE CONTINUOUS PHASE MODULATIONS

by

D.J. Vaisey

P.J. McLane

Report No. 82-3

Final Report - Part II

Prepared for

The Department of Communications

Under DSS Contract No. OSU81-00246

Department of Electrical Engineering

Queen's University

Kingston, Ontario, Canada

ABSTRACT

The use of Butterworth and Chebychev low pass filters as the receive filters in suboptimum in-phase (I) and quadrature-phase (Q) receivers is considered for several bandwidth-efficient modulations. These modulations are: Minimum Shift Keying (MSK), Tamed Frequency Modulation with Rectangular Pulse Shaping (TFMREC), and MSK with duobinary encoding of the source bits (DMSK). The sensitivity of the modulations with their I and Q receivers to a noisy phase reference and to timing errors is also investigated. It is found that the standard low pass filter receive filters perform quite well when compared to other much more complicated filters. The use of standard filters should thus be considered in any system design. The modulations, with their simple receivers, can be ranked according to sensitivity to a noisy phase reference and timing errors as follows: MSK, DMSK, TFMREC; MSK has the least sensitivity. This ordering is the inverse of the one for the best bandwidth efficiency.

TABLE OF CONTENTS

LIST OF FIGURES

LIST OF TABLES

SUMMARY OF NOTATION

Symbols:

$\underline{a}$	- the transformation of $\underline{\beta}$; $\beta_k \in \{0,1\}$, $a_k \in \{-1,1\}$
A	- the amplitude of the CPM signal
$\underline{b}$	- the sequence at the output of the correlator
B	- the two-sided 3 dB filter bandwidth
D	- the delay operator
dB	- decibel
d_{min}	- the normalized Euclidean distance
$E(\cdot)$	- the expectation operator
$F^{-1}(\cdot)$	- the inverse Fourier transform operator
F(D)	- the partial response polynomial
g(t)	- the frequency pulse of the modulator
h	- the modulation index
h(t)	- the impulse response of the receive filter
H(f)	- the Fourier transform of h(t)
ℓ	- $\max\ n-k : \gamma + t_k > nT$
L	- the duration of the pulse response in bit intervals

m	-	the number of possible states
M	-	the number of T length basic pulses
$n(t)$	-	additive Gaussian bandpass noise
$n_1(t), n_2(t)$	-	additive baseband Gaussian noise
$n'_1(t), n'_2(t)$	-	the baseband noise after the receive filter
N	-	the number of possible waveforms
$p_i(t)$	-	one of the T length basic pulses
$P_i(f)$	-	the Fourier transform of $p_i(t)$
$p_{\tilde{\theta}}(\tilde{\theta})$	-	the pdf of $\tilde{\theta}$
Pe	-	the probability of a bit error
$q(t)$	-	the phase pulse of the modulator
$r_I(t)$	-	the output of the receive filter in the I channel
$r_Q(t)$	-	the output of the receive filter in the Q channel
$R_{n'_1}(\tau)$, $R_{n'_2}(\tau)$	-	the autocorrelation function for $n'_1(t)$ and $n'_2(t)$
$s(t)$	-	the CPM signal
$S_n(f)$	-	the power spectrum of $n(t)$
$S_{n_1}(f), S_{n_2}(f)$	-	the power spectrum of $n_1(t)$ and $n_2(t)$
$S_{n'_1}(f)$, $S_{n'_2}(f)$	-	the power spectrum of $n'_1(t)$ and $n'_2(t)$
t_k	-	the sampling point for the k_{th} bit
T	-	the bit interval [seconds/bit]

$u_i(t)$	-	the input to the receive filter for the i_{th} waveform
$w(t)$	-	additive white Gaussian noise
W	-	half the bandwidth of the IF filter
$x(t)$	-	the input to the receiver
$\underline{\alpha}$	-	the source bit sequence
$\underline{\hat{\alpha}}$	-	the estimate of the source bit sequence
$\underline{\beta}$	-	the sequence after the differential encoder
$\delta(t)$	-	the Dirac delta function
σ_n^2	-	the variance of $n(t)$
$\sigma_{n_1}^2, \sigma_{n_2}^2$	-	the variance of $n_1(t)$ and $n_2(t)$
σ_n^2,	-	the variance of $n_1'(t)$ and $n_2'(t)$
γ	-	the sampling offset
θ	-	the phase offset of $x(t)$
$\hat{\theta}$	-	the phase of the carrier reference
$\tilde{\theta}$	-	$\theta - \hat{\theta}$
Δ	-	the timing offset
μ	-	the phase reference signal to noise ratio
$*$	-	the convolution operator
$\oplus$	-	the exclusive OR operator

Abbreviations:

AM/AM	-	amplitude modulation to amplitude modulation

AM/PM	-	amplitude modulation to phase modulation
BPSK	-	binary phase shift keying
CPM	-	continuous phase modulation
DMSK	-	duo-binary MSK
FFT	-	fast Fourier transform
I	-	in phase
ISI	-	intersymbol interference
MSK	-	minimum shift keying
pdf	-	probability density function
Q	-	quadrature phase
QPSK	-	quaturnary phase shift keying
OQPSK	-	offset QPSK
SNR	-	signal-to-noise ratio
TFM	-	tamed frequency modulation
TFMREC	-	TFM with rectangular pulse shaping
Receiver 1	-	the deBuda receiver
Receiver 2	-	the receiver on p.39

CHAPTER 1

INTRODUCTION

The purpose of this study is to investigate some simple receivers for certain bandwidth-efficient modulations that have a constant envelope. Bandwidth-efficient modulations are important due to the increasing demand for communication services and the fact that the available bandwidth is limited. For reasons of efficiency the power amplifier in radio communications equipment is usually operated near power saturation resulting in a non-linear amplification. Any amplitude variations in the input to this amplifier will thus result in AM/AM and AM/PM distortion as well as spectral spreading. It is thus desirable for the input to the amplifier to have a constant envelope. At present, the area of bandwidth-efficient modulations with a constant envelope is the subject of much research.

Continuous phase modulation (CPM) with partial response encoding of the source bits is a modulation technique that has both bandwidth efficiency and a constant envelope. The

correlation of the bits introduced by the partial response encoding introduces controlled intersymbol interference (ISI) and smooths the phase of the signal. The amount of smoothing is a determining factor in the spectral efficiency of the modulation [1]. In this scheme coding and modulation techniques are used in tandem.

Optimal decoding of the general CPM scheme requires maximum likelihood decoding. The Viterbi algorithm performs maximum likelihood detection and its use in decoding CPM signals has been described by Aulin [2]. With the Viterbi algorithm the number of possible states in the decoder can become quite large, making the implementation of the receiver very complicated. It is thus desirable to find simpler, and hence suboptimal, detectors for CPM.

If the modulation index of the CPM scheme equals one-half, it is possible to decode the signal using a receiver with an in phase (I) and quadrature phase (Q) arm detector [3]. If the two arms of the detector are uncoupled then the receiver is inherently suboptimal in CPM schemes where the I and Q channel waveforms are not independent. The arm filters of the receiver must be chosen to yield the best possible suboptimal performance; there are several strategies for doing this. If the filters are constrained

to be linear, then, under this constraint, it is possible to choose them optimally [17]. The baseband I and Q waveforms can be broken up into a set of characteristic pulse shapes, each with the duration of the sampling interval. The arm filters can then be chosen to be the filters matched to the pulse shape of least energy. Alternatively, the arm filters can be matched to the average waveform [4], giving optimal results as the signal to noise ratio (SNR) vanishes, or to an approximation of the eye pattern [5].

Easily realizable filters such as Butterworth and Chebychev low pass filters can also be used as the arm filters in the suboptimal receiver. These filters degrade the performance from that obtained with more complicated filters; however, in many cases this degradation may not be too significant. Also, the more complicated filters that are matched to certain waveshapes tend to be more sensitive to channel distortion than an initially mismatched filter [6]; they are also often much more difficult to realize.

This study investigates the effects of using standard low pass filters as the arm filters of I and Q receivers for certain CPM modulations. The sensitivity of these systems to a noisy phase reference and timing errors is

also examined. All of the CPM schemes investigated have modulation indices equal to one-half; they are: Minimum Shift Keying (MSK), Tamed Frequency Modulation (TFM) with rectangular pulse shaping (TFMREC), and MSK with Lender's [7] duo-binary encoding of the source bits (DMSK). MSK is a standard modulation and it is used as a benchmark to compare the others. The type of I and Q receiver used for each of the modulations is the deBuda type receiver [8]. However, an alternative receiver is also presented for DMSK that can resolve a 90° phase ambiguity in its carrier reference at the cost of increased sensitivity to noise and distortion; the deBuda receiver can resolve a 180° phase ambiguity. The filter types used in the study are: second order Butterworth filters, fourth order Chebychev filters with 0.1 dB ripple, and sixth order Butterworth filters. The optimum filter type and the corresponding best bandwidth is found for each modulation scheme.

1.1 The System Model

A block diagram of the communications system studied in this report is shown in Fig. 1.1. The output of the source is an infinitely long binary sequence $\underline{\alpha} = (\ldots, \alpha_{-1},$

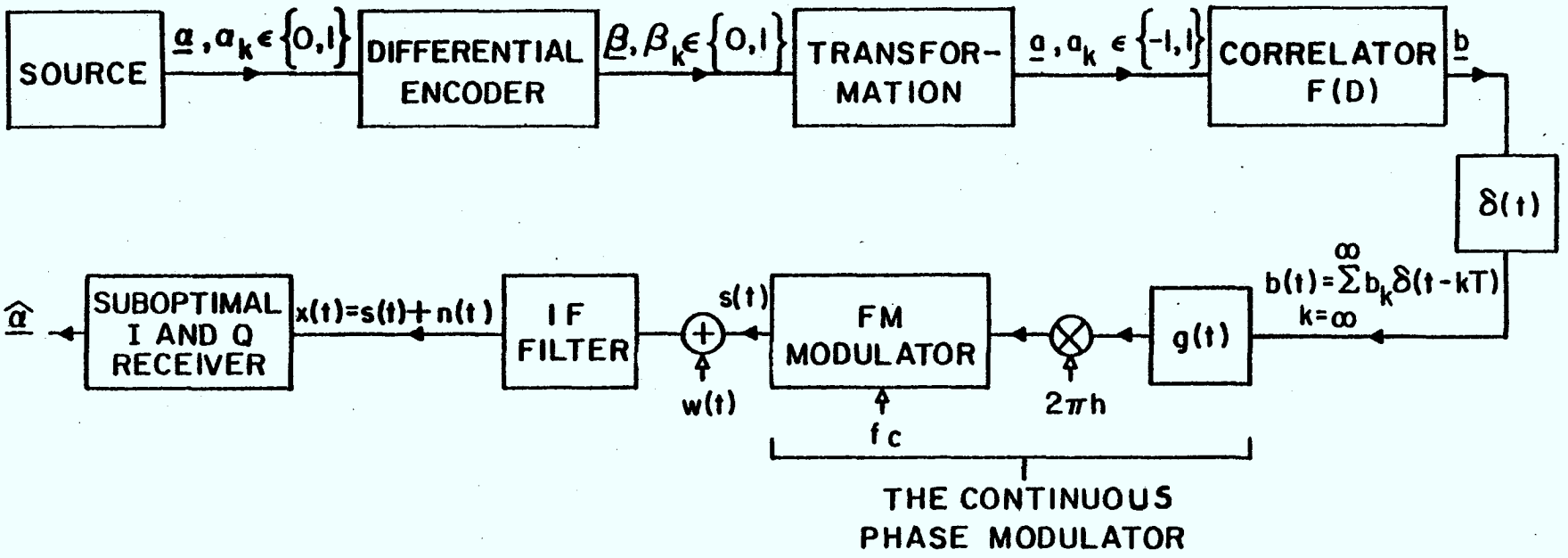

Figure 1.1 : The System Model

$\alpha_0, \alpha_1, \ldots)$; each symbol takes on the value "0" or "1" with equal probability. The source bits are then differentially encoded; this must be done for the receivers in this thesis to work properly. The output of the differential encoder is the sequence $\underline{\beta} = (\ldots, \beta_{-1}, \beta_0, \beta_1, \ldots)$ with $\beta_k \in \{0,1\}$. The sequence $\underline{\beta}$ is then mapped into another sequence $\underline{a}$ such that if $\beta_k = 0$ then $a_k = -1$, and if $\beta_k = 1$ then $a_k = 1$. After the mapping the elements of $\underline{a}$ are correlated with each other in a partial response encoder [9]. The correlated sequence is $\underline{b} = (\ldots, b_{-1}, b_0, b_1, \ldots)$, and

$$\sum_{k=-\infty}^{\infty} b_k \, \delta(k - kT),$$

where $\delta(t)$ is the Dirac delta function, is applied to the continuous phase modulator. White Gaussian noise with double sided power spectral density $N_0/2$ is added to the modulator output. The combined signal then passes through an IF filter with centre frequency f_c, the carrier frequency, and bandwidth 2W. The filter bandwidth is wide enough not to distort the signal; however, the noise process is filtered into bandpass noise. The signal is then received, and estimates made of the source bits α_k. The estimate sequence is $\underline{\hat{\alpha}} = (\ldots, \hat{\alpha}_{-1}, \hat{\alpha}_0, \hat{\alpha}_1, \ldots)$.

The bandpass noise can be written as [10]

$$n(t) = n_1(t)\cos(2\pi f_c t) - n_2(t)\sin(2\pi f_c t) \qquad (1)$$

where $n_1(t)$ and $n_2(t)$ are independent baseband Gaussian noise process with

$$S_{n_1}(f) = S_{n_2}(f) = \begin{cases} N_0 & |f| \leq W \\ 0 & \text{elsewhere} \end{cases} .$$

$S_{n_1}(f)$ and $S_{n_2}(f)$ are the power spectra of $n_1(t)$ and $n_2(t)$ respectively. The variance of the noise processes will be

$$\sigma_n^2 = \sigma_{n_1}^2 = \sigma_{n_2}^2 = 2 N_0 W .$$

1.2 The General CPM Scheme

It is possible to write a general expression for the constant envelope CPM signals s(t). The expression is

$$s(t) = A\cos[2\pi f_c t + \phi(t)] \qquad (2)$$

where $A = \sqrt{2E_b/T}$, E_b is the energy transmitted per bit, T is the reciprocal of the bit rate, and $\phi(t)$ is the information-carrying phase. The phase term can be broken

down as follows:

$$\phi(t) = 2\pi h \sum_{k=-\infty}^{\infty} b_k \, q(t - kT)$$

where h is the modulation index, and $q(t)$ is the phase response (phase pulse) of the modulator. The output of the correlator, $\underline{b}$, is determined by the partial response polynomial $F(D)$, where D is the delay operator defined by

$$a_{n+k} = a_n \, D^k \quad .$$

$F(D)$ is defined by

$$F(D) = \frac{\sum_{n=0}^{m} f_n \, D^n}{\sum_{n=0}^{m} f_n} \tag{3}$$

where f_n is a real number. The division in (3) is necessary for normalization so that schemes which are identical except for different partial response polynomials will have the same maximum phase excursion per bit interval. The output of the correlator will be

$$b_k = a_k \, F(D) \quad .$$

The phase response can in turn be defined by the frequency response (frequency pulse) g(t); ie:

$$q(t) = \int_{-\infty}^{t} g(\tau)\, d\tau \quad .$$

In practical modulations g(t) must be time limited; using this and the fact that the system must be causal

$$g(t) = 0 \qquad t \leq 0 \quad , \quad t \geq L$$

where L is a finite number. Also, for normalization purposes

$$\int_{0}^{L} g(t)\, dt = \frac{1}{2} \quad .$$

The above implies that

$$q(t) = \begin{cases} 0 & t \leq 0 \\ \\ \frac{1}{2} & t \geq L \quad . \end{cases}$$

The nature of g(t) and F(D) determine the smoothness of the phase of s(t) and thus are also significant in determining the spectral properties of the modulation. In

general, the smoother the phase of the modulation the more rapidly the power spectrum falls off. Baker [1] has shown that the power spectrum decreases as

$$|f|^{-(2y + 2)}$$

where y is the number of continuous derivatives of $g(t)$.

1.3 Literature Review

The class of bandwidth-efficient constant envelope modulations has been an area of much recent research. These signals can all be written in the form $s(t) = A \cos[\omega_c t + \phi(t)]$ where $\phi(t)$ follows a coded pattern in response to the data. Anderson et al. [11] have shown that modulation codes of this class can approximate any power-bandwidth combination consistent with Shannon's Gaussian channel capacity. However, Anderson cautions that efficient signals have an exact synchronization requirement resulting in a trade-off between performance and receiver complexity. The class of CPM schemes is a sub-class of the above general class of schemes.

CPM schemes with and without partial response encoding of the bits has been studied by Aulin et al [12] [13]; maximum likelihood detection of the received signal

is used in both investigations. A good explanation of general partial response techniques is given by Kabal and Pasupathay [9]. In [12] Aulin gives the performance and the power spectra of full response CPM schemes with different modulation indices. Aulin [13] then includes partial response encoding of the source data in order to improve the spectral performance; receiver and transmitter implementations are also discussed and it is found that an almost rational h is necessary for the modulation to be easily implemented.

A numerical method for finding the spectral properties of partial response CPM signals has been given by Deshpande and Wittke [14]; the power spectrum is computed for several examples. Aulin et al. [15] have examined the effect of changing the frequency response pulse, $g(t)$, in CPM signals. Pulses of length $2T$ with different numbers of continuous derivatives are studied and the trade-off between spectrum and performance examined. Deshpande and Wittke [16] have developed a technique to find the T-length frequency pulse that results in the smallest out of band power for the binary full response case. Lower bounds on the maximum band efficiency obtainable by choosing different T length frequency pulses were found for the $h = 1/2$ scheme.

Galko and Pasupathay [23] have developed a method for

finding the optimal linear receiver for digital signals. Their linear receiver divides the signal space up into M regions separated by linear boundaries, where M is the number of hypotheses. Galko and Pasupathay [17] have applied this theory to find linear receive filters for I and Q receivers used to demodulate binary CPM schemes with $h = 1/2$; they observe the I and Q channel waveforms over L bit intervals and take each possible waveform as a point in the signal space. The signal space is divided up into two decision regions: one for the signals with a positive value at the sampling point, and another for signals with a negative value. The optimum linear receiver is then found to make the decision. The performance of this receiver is found to be quite close, within a fraction of a decibel, to the performance of the maximum likelihood receiver. Aulin et al [3] have examined the performance of I and Q receivers for the above modulations using different types of arm filters; two used are: a filter based on the average waveform, and a filter matched to the minimum energy baseband pulse shape.

MSK is a CPM modulation with $h = 1/2$ that has received quite a bit of attention for its use with bandlimited channels [18]. MSK is a linear modulation, even though it

is generated in a non-linear manner, and has been shown to be a special case of Offset Quadrature Phase Shift Keying (OQPSK) with sinusoidal symbol weighting [19]. deBuda [8] has devised an optimal coherent I and Q receiver for MSK that is easy to build. The receiver is only optimal if arm filters matched to the MSK baseband pulse are used; however, other filters may achieve a performance level that is close to the optimum. Since MSK is linear, Prabhu [20] has been able to find an analytical method to determine the degradation in performance suffered by MSK when it is bandlimited. Prabhu found that for severe bandlimiting MSK is inferior to OQPSK, while for slight bandlimiting MSK is a little bit better than OQPSK.

TFM is a CPM scheme with h = 1/2 developed for use in digital mobile radio [5]. TFM uses a correlator that correlates three source bits together and a non-rectangular frequency pulse to obtain spectral economy. DeJager and Dekker [5] describe the operation of TFM and present the results of a test implementation. A deBuda-type receiver is used in this implementation.

Rhodes [21] has developed a spectrally efficient constant envelope modulation called Frequency Shift Offset Quadrature Modulation (FSOQ). FSOQ is spectrally equivalent

to DMSK, but is generated as a form of OQPSK. Rhodes has simulated FSOQ in a channel with the characteristics of INTELSAT IV. It is concluded that FSOQ requires twenty percent less bandwidth than MSK for good performance.*

Jones [6] has considered the replacement of matched filters in an I and Q receiver for QPSK by standard two pole Butterworth low pass filters. The performance degradation with the change was quite small. Jones's best Butterworth filter had a BT product of 0.5, where B is the two sided 3 dB filter bandwidth. McCreath and McLane [22] have laid out an optimization procedure to find the best bandwidth and sampling time for Butterworth and Chebychev receive and transmit filters for a Binary Phase Shift Keying (BPSK) system; both linear and non-linear channels were considered.

Rhodes [30] has calculated the effects of a noisy phase reference on BPSK, OQPSK, and QPSK schemes. Matyas [29] has extended this work to include MSK. The schemes can be written in order of decreasing sensitivity to a noisy phase reference as: BPSK, MSK, OQPSK, QPSK.

---

*DMSK has the same performance as FSOQ for an additive white Gaussian Noise Channel.

1.4 Presentation Outline

The system model and the general expression for continuous phase modulated signals has been presented in Chapter 1. The specific modulations used in this report and their I and Q receivers are discussed in Chapter 2. In Chapter 3 the use of Butterworth and Chebychev low pass filters as the receiver filters is considered. The optimum low pass filter is found for each of the modulations and the results compared to those obtained when other types of receive filters are used. The effects of a noisy phase reference on the performance of the modulations is considered in Chapter 4 and that of timing errors in Chapter 5. Finally, conclusions and suggestions for further work are given in Chapter 6.

CHAPTER 2

A DESCRIPTION OF THE MODULATION SCHEMES

The results in this report are given for three specific modulation schemes: MSK, DMSK and TFMREC. The power spectra for these modulation schemes, and that for QPSK, are plotted in Fig. 2.1. The bandwidth efficiency, minimum Euclidean distance, and performance loss between the modulations when maximum likelihood decoding is used are given in Table 2.1 [14]. A description of the three modulation schemes of interest and receivers for them follows.

Type of Modulation	Efficiency bits/sec/Hz		Normalized Minimum Euclidean Dist. d_{min}.	10 log $\frac{d^2 \text{ min}}{d^2 \text{ min}}$ (MSK)
	99% power	99.9% power		
QPSK	0.1	0.01	$\sqrt{2.0}$	0.0
MSK	0.85	0.36	$\sqrt{2.0}$	0.0
DMSK	1.09	0.56	$\sqrt{1.73}$	-0.63
TFMREC	1.25	0.79	$\sqrt{1.45}$	-1.30

Table 2.1: A Comparison of the Modulations

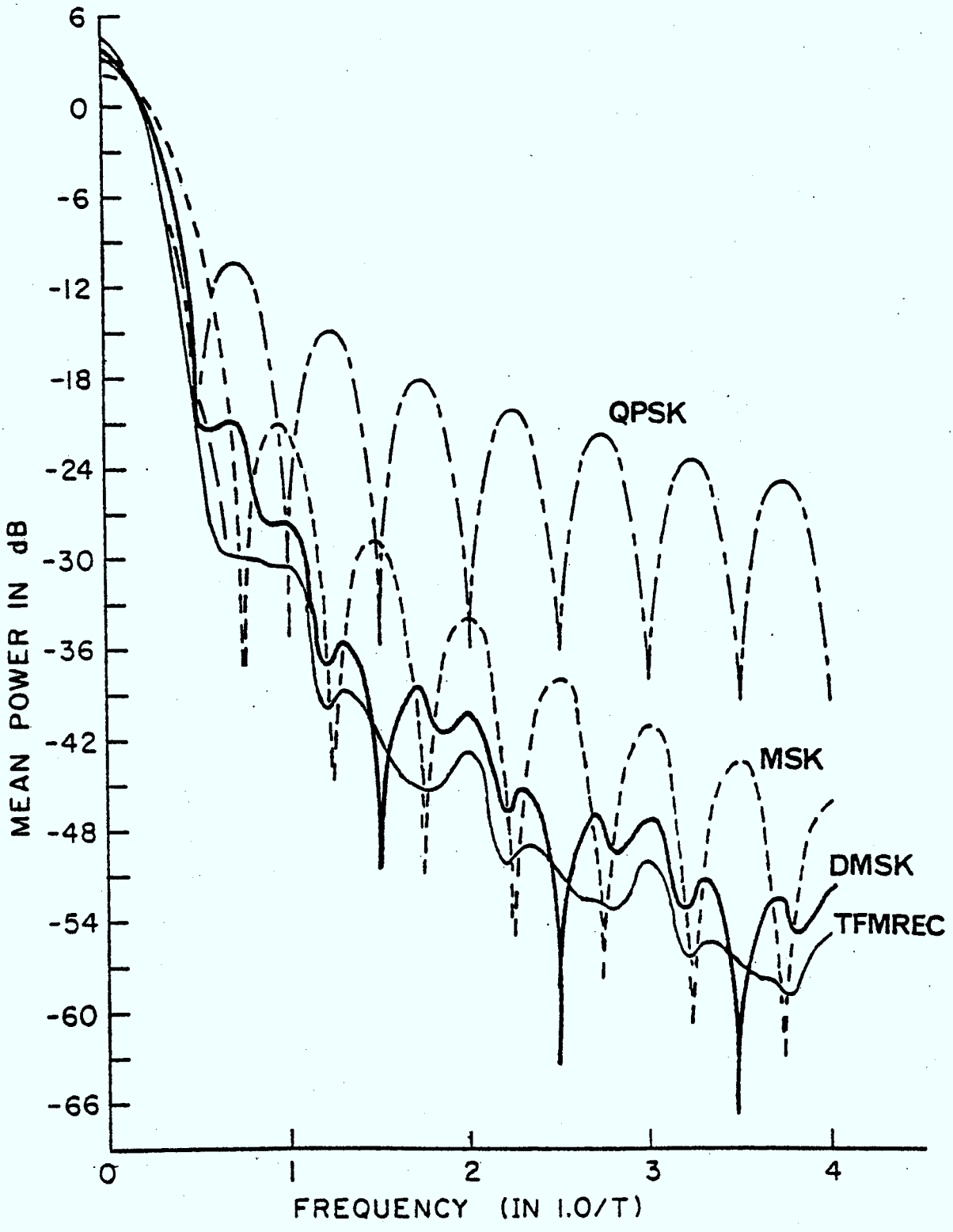

Figure 2.1 : The Power Spectra of the Modulations

2.1 A Description of MSK

A frequency shift keyed (FSK) signal with modulation index h = 1/2 has a continuous phase; this special case of FSK is termed MSK. Due to its continuous phase MSK is also a CPM scheme and can be written in the form of (2). MSK has no partial response encoding making F(D) = 1, and $b_k = a_k$. Therefore,

$$\phi(t) = \pi \int_{-\infty}^{t} \sum_{k=-\infty}^{\infty} a_k \, g(t - kT)dt \qquad (4)$$

Also, for MSK

$$g(t) = \begin{cases} \frac{1}{2T} & 0 < t < T \\ 0 & \text{elsewhere} \end{cases} .$$

Therefore,

$$\phi(nT) = \frac{\pi}{2} \sum_{k=-\infty}^{n-1} a_k \quad , \qquad (5)$$

where n is an integer.

If $\phi(t)$ is considered modulo 2π then it can take on only four possible values at the ends of the bit intervals;

these values are: 0, $\pi/2$, π, and $3\pi/2$ radians. By observing (5) it is seen that the phase increases by $\pi/2$ radians during the kth bit interval if $a_k = 1$, and decreases by $\pi/2$ radians if $a_k = -1$. By examining (4) it is seen that this phase change occurs linearly. The phase behaviour of all possible MSK signals is thus easily described by a phase tree. The tree with $\phi(0) = 0$ radians is shown in Fig. 2.2.

One of the most important properties of MSK is that, if $\phi(0)$ is initially 0 or π radians then

$$\phi(2k) \in \{0,\pi\} \bmod 2\pi$$
$$\phi(2k+1) \in \{\pi/2, -\pi/2\} \bmod 2\pi$$

where k is a positive integer. This property is easily seen to be true when Fig. 2.2 is examined. The phase of MSK thus exhibits what shall be termed the half plane property: at even bit times the decision regions for $\phi(t)$ in the phase plane are the two half planes separated by the imaginary axis while at odd bit times the decision regions are separated by the real axis. This half plane property will also appear in the subsequent modulations.

A receiver that utilizes the half plane property of MSK has been presented by deBuda [8]. At even bit times,

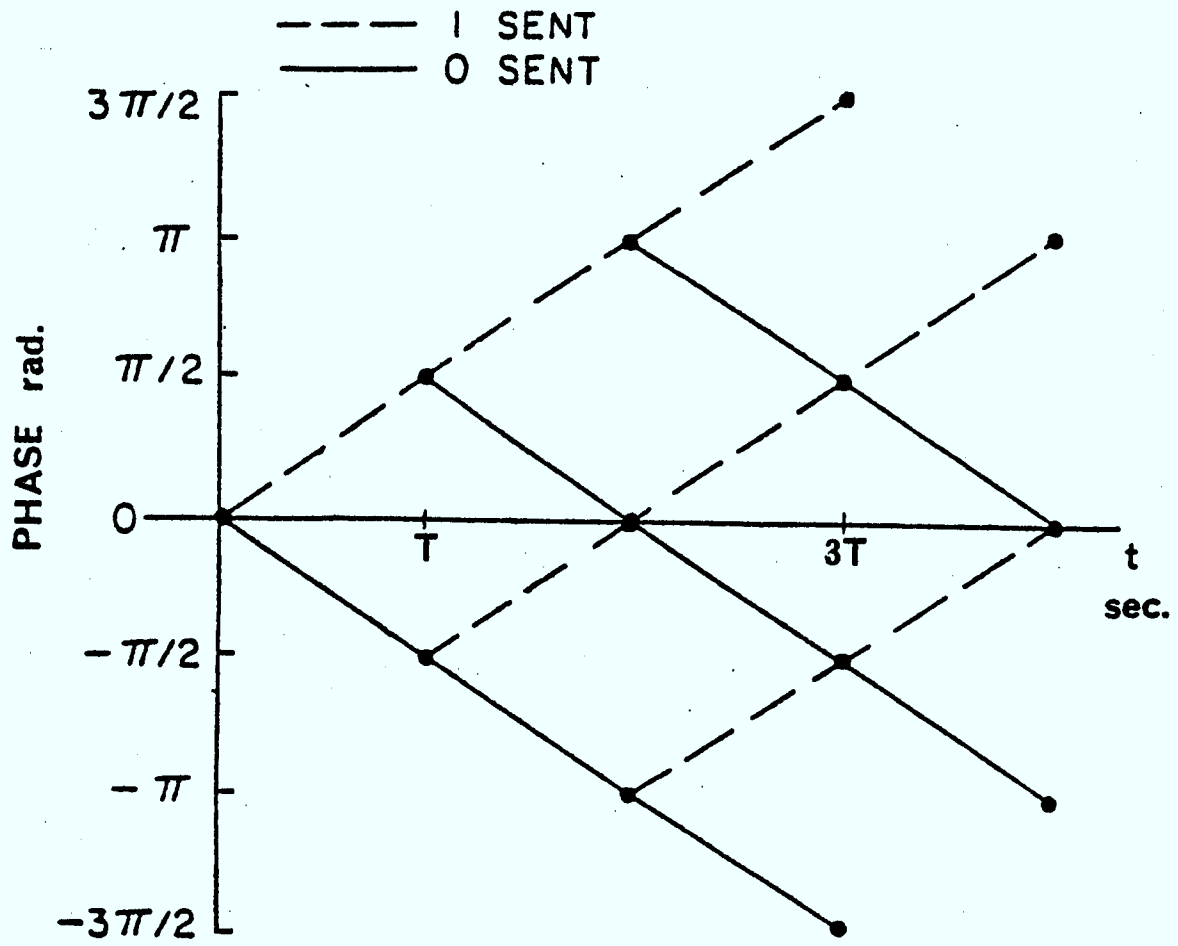

Figure 2.2 : The Phase Tree for MSK

deBuda's receiver determines whether the phase is 0 or π radians with an I channel decision. If the I channel output is positive then the decision is that the phase is in the right half plane; if it is negative, then the decision is that the phase is in the left half plane. Similarly, the Q channel is used to determine whether the phase is $\pi/2$ or $-\pi/2$ radians at odd bit times by making a decision on the top or bottom plane. A phase error results when the I , or Q , channel output causes the decision to be made on the wrong half plane. A block diagram of deBuda's receiver is given in Fig. 2.3. Techniques for implementing the carrier and timing recovery circuits are given in [8].

A receiver such as deBuda's gives out transition information about the data bit sequence $\underline{a}$; that this is so can be seen by considering the phase difference

$$\phi(kT) - \phi[(k + 2)T] \quad .$$

This difference has only two possible values: 0 , and π radians. If the difference is π radians then a_{k+1} must be equal to a_k, while if it is 0 radians then a_k and a_{k+1} must be opposite. Thus, at $t=(2k+2)T$ the output of the I channel exclusive OR gate in Fig. 2.3 will be high if

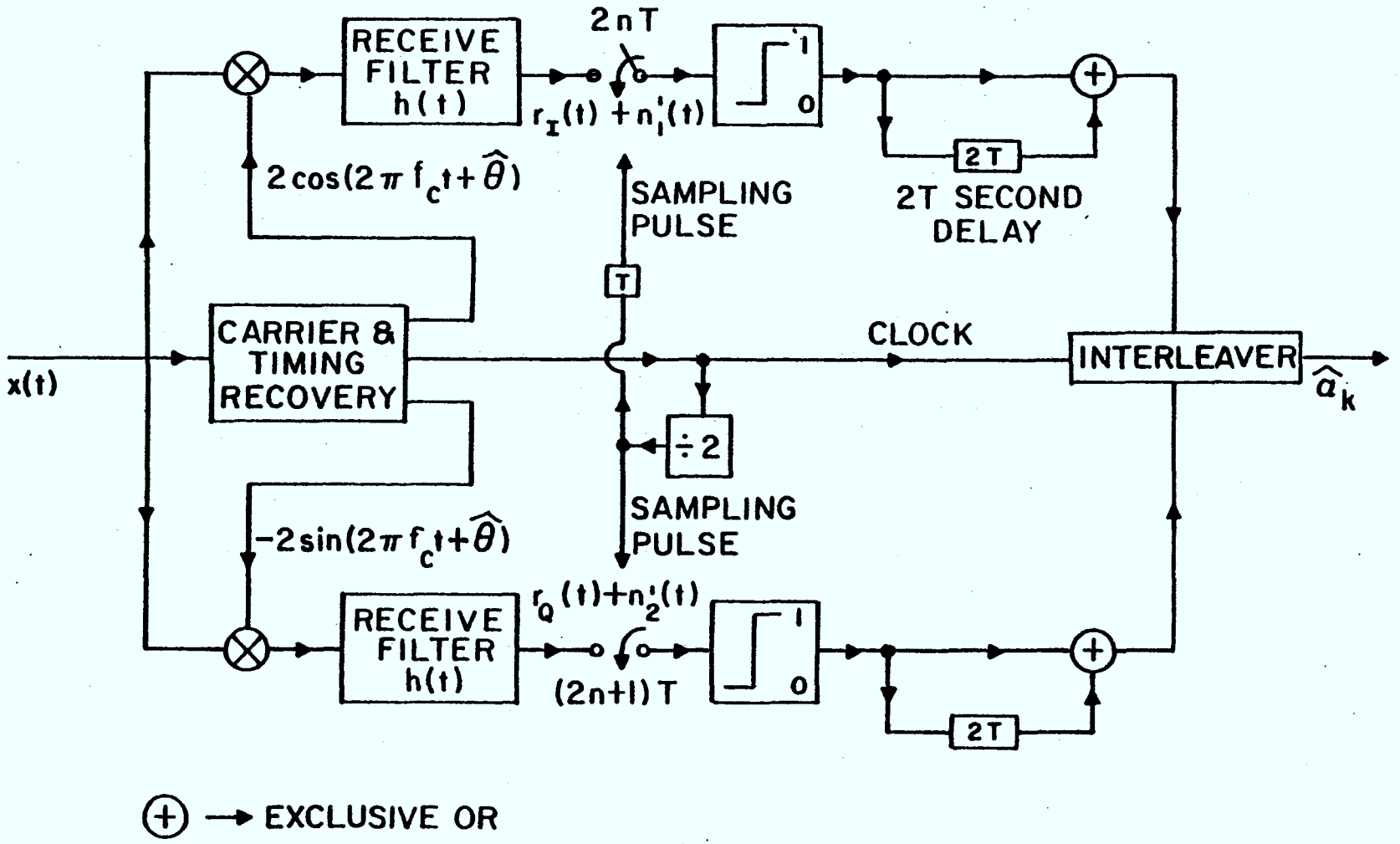

Figure 2.3 : The deBuda Receiver

$a_{2k} = a_{2k+1}$, and low if $a_{2k} \neq a_{2k+1}$. The results are similar for the Q channel at odd bit times.

The source bits can be obtained at the receiver output if they are differentially encoded prior to the mapping to the $\underline{a}$ sequence. This encoding operation is shown in Fig. 1.1 and can be written mathematically as

$$\beta_{k+1} = \overline{\alpha_k \oplus \beta_k}$$

where $\oplus$ denotes exclusive OR, and the bar denotes the complement operation. Thus, $\beta_{k+1} \neq \beta_k$, and hence $a_{k+1} \neq a_k$, implies that $\alpha_k = 0$; $\beta_{k+1} = \beta_k$ implies that $\alpha_k = 1$.

The interleaver in Fig. 2.3 recreates an estimate of the source stream from the output of the I and Q channels. It should be noted that due to the memory involved in the differential encoding, an error in detecting a transition, a phase error, will result in a double error in the source stream estimate. Thus, ignoring the small probability of multiple phase errors in a row, the probability of error is effectively doubled.

2.2 A Description of TFMREC

TFM is a CPM scheme with h = 1/2 that has very good spectral efficiency. This spectral efficiency is obtained

correlating the bits before modulation and then using a non-rectangular g(t) that provides extra smoothing of the phase. For TFM [3]

$$g(t) \simeq \frac{1}{2T}\left[\frac{\sin(\frac{\pi t}{T})}{\frac{\pi t}{T}} - \frac{\pi^2}{24} \cdot \frac{2\sin(\frac{\pi t}{T}) - \frac{2\pi t}{T}\cos(\frac{\pi t}{T}) - (\frac{\pi t}{T})^2\sin(\frac{\pi t}{T})}{(\frac{\pi t}{T})^3}\right],$$

and

$$F(D) = \frac{1 + 2D + D^2}{4}$$

$$b_k = (a_k + 2a_{k-1} + a_{k-2})/4 \quad .$$

If g(t) is now made into a rectangular pulse,

$$g(t) = \begin{cases} \frac{1}{2T} & 0 \leq t \leq T \\ 0 & \text{elsewhere}, \end{cases}$$

but the same modulation index and F(D) are kept, then a different CPM scheme is obtained. This modulation is termed TFMREC. The spectral efficiency of TFMREC is less than that of TFM, but it is still quite good and the resulting

modulation much simpler.

The correlation of the source bits causes the phase changes to be smoothed; however, the number of points in the signal constellation increases to eight increasing the sensitivity to noise. It should be noted that the signal constellations of TFM and TFMREC are identical; only the form of the transitions between points in the constellation changes.

In both TFM and TFMREC there are certain phases that are allowed at the end of even, and odd, bit intervals while others are not possible. The state of the modulation at the start of the k_{th} bit interval is defined as

$$[\phi(kT), \alpha_{k-2}, \alpha_{k-1}] \quad .$$

The allowed and forbidden states are the same for both TFM and TFMREC. The allowed states when k is even and odd are shown in Figures 2.4(a) and 2.4(b) respectively. In these figures it is assumed that the initial state of the modulation was in one of the "allowed" states. In Fig. 2.5(a) and Fig. 2.5(b) the phase transitions resulting from the bits α_k and α_{k+1} are shown; all possible initial states are considered. It can be seen from Figures 2.5(a) and 2.5(b) that the modulation is always in one of the allowed

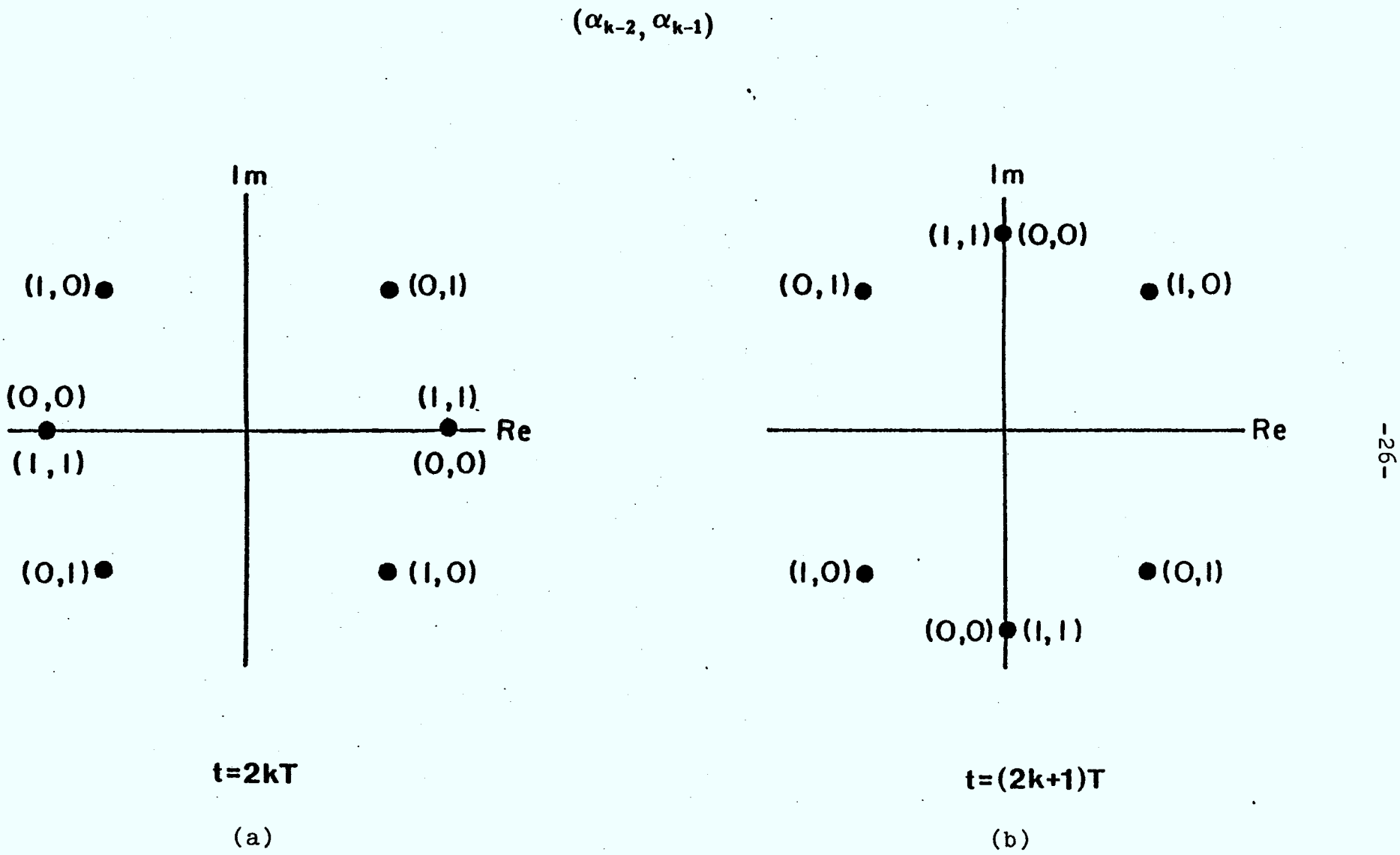

Figure 2.4 : The Allowed States for TFMREC

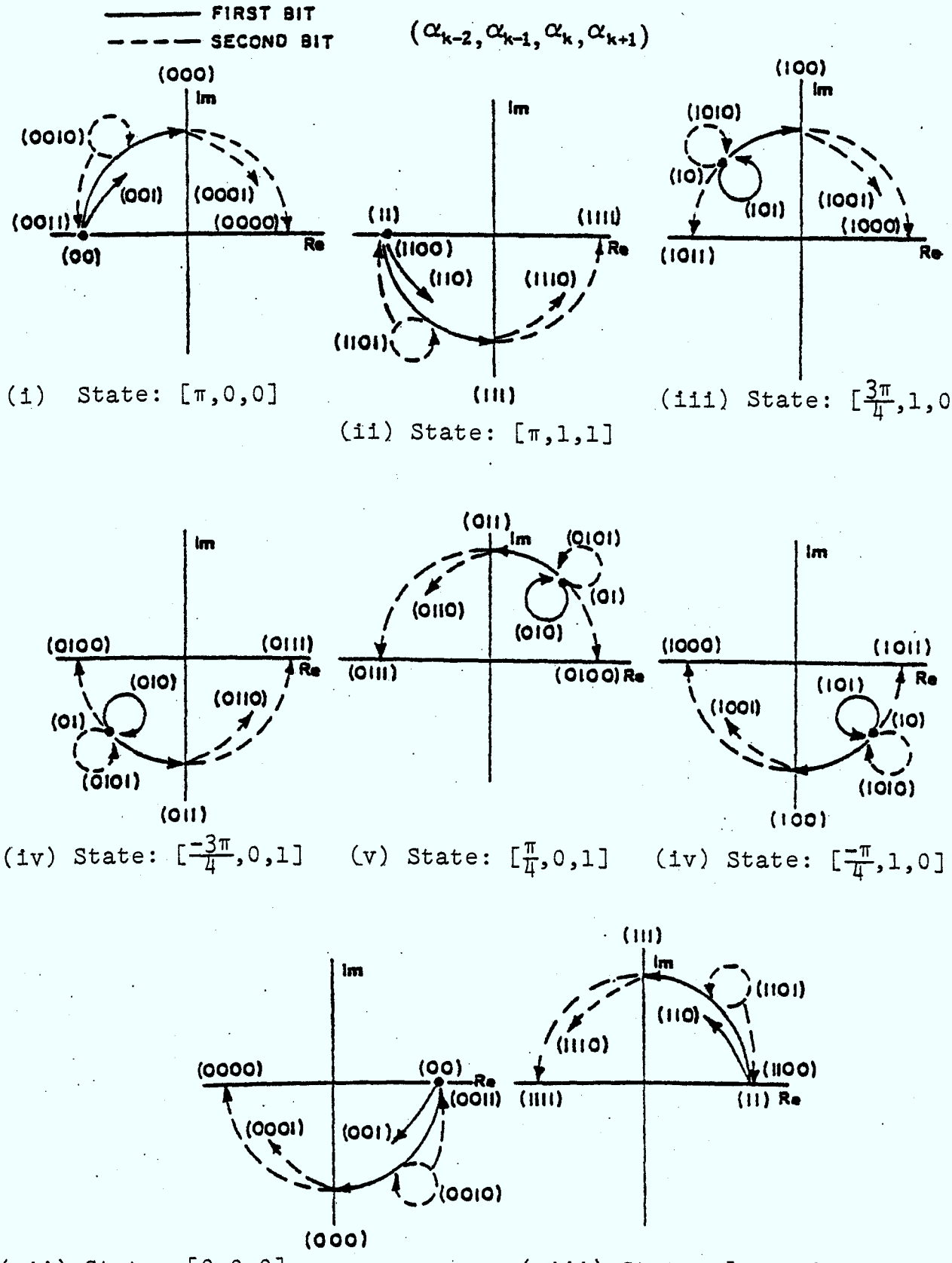

(i) State: $[\pi,0,0]$

(ii) State: $[\pi,1,1]$

(iii) State: $[\frac{3\pi}{4},1,0]$

(iv) State: $[\frac{-3\pi}{4},0,1]$

(v) State: $[\frac{\pi}{4},0,1]$

(iv) State: $[\frac{-\pi}{4},1,0]$

(vii) State: $[0,0,0]$

(viii) State: $[0,1,1]$

Figure 2.5(a) : The Phase Transitions for TFMREC Starting at an Even Bit Time

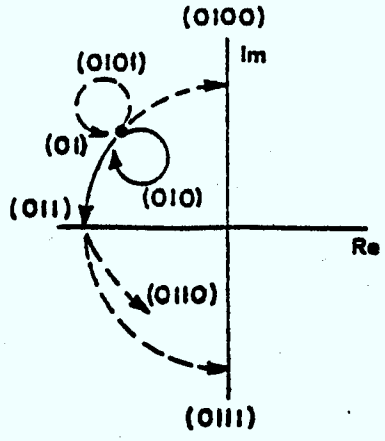

(i) State: $[\frac{3\pi}{4},0,1]$

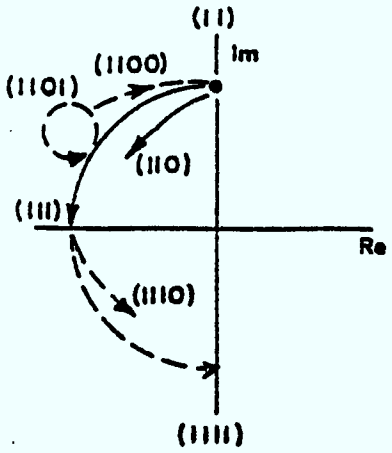

(ii) State: $[\frac{\pi}{2},1,1]$

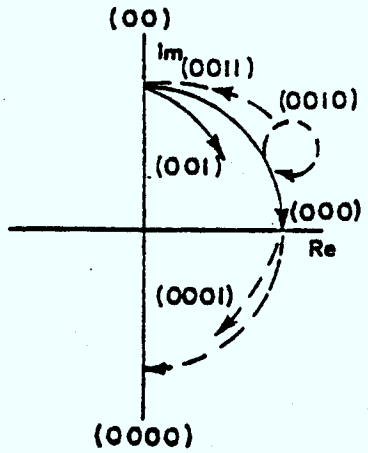

(iii) State: $[\frac{\pi}{2},0,0]$

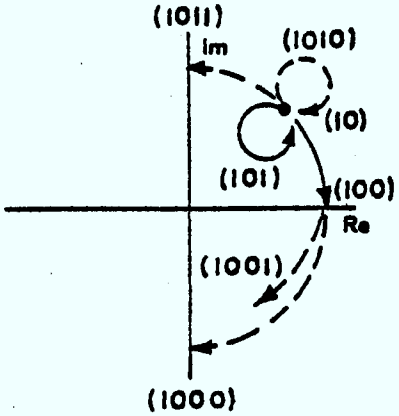

(iv) State: $[\frac{\pi}{4},1,0]$

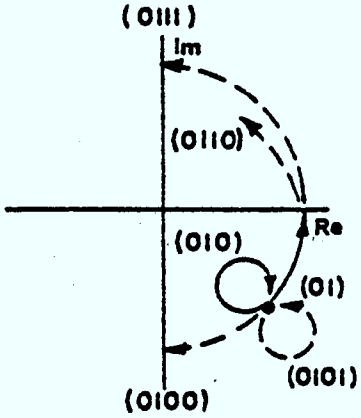

(v) State: $[\frac{-\pi}{4},0,1]$

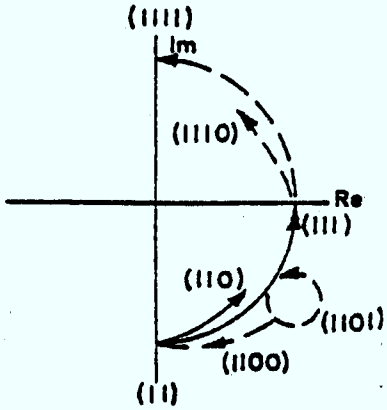

(vi) State: $[\frac{-\pi}{2},1,1]$

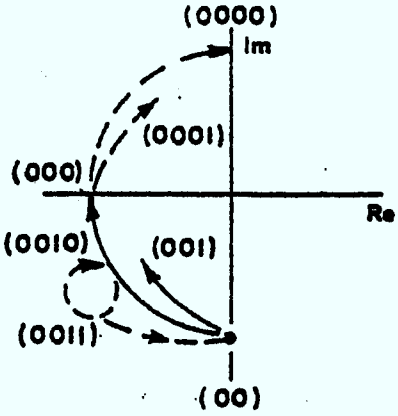

(vii) State: $[\frac{-\pi}{2},0,0]$

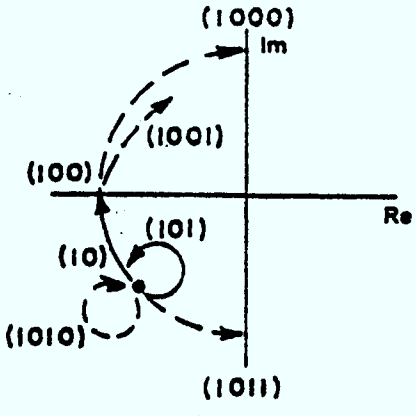

(viii) State: $[\frac{-3\pi}{4},1,0]$

Figure 2.5(b) : The Phase Transitions for TFMREC Starting at an Odd Bit Time

states at $t = kT$ no matter what the value of k .

From Figures 2.5(a) and 2.5(b) it can be seen that TFMREC, and TFM, has the same half plane property discussed earlier for MSK. It is also evident that $\alpha_k = \alpha_{k-1}$ implies that $\phi(kT)$ and $\phi[(k+2)T]$ are in opposite half planes, and that $\phi(kT)$ and $\phi[(k+2)T]$ in the same half plane implies that $\alpha_k \neq \alpha_{k-1}$. Thus, it is possible to demodulate TFMREC, and TFM, using a deBuda type receiver; however, the optimum receiver arm filters will be different in the MSK, TFM, and TFMREC receivers. As in MSK the source bits must be differentially encoded for estimates of them to come out of the receiver. Also, a phase error results in a double error in the source bit estimate.

Another property of TFMREC, and TFM, is that energy is transmitted at the carrier frequency; this does not happen in MSK. The pure carrier is transmitted when $b_k = 0$ which, for independent data, occurs one quarter of the time. Thus, better carrier recovery schemes should exist for TFMREC than for MSK.

2.3 A Description of DMSK

DMSK uses duobinary encoding [7] of the source bits before they are applied to a MSK modulator. Duobinary encoding gives a better bandwidth efficiency than any other

partial response scheme that correlates two bits [14]. For DMSK:

$$F(D) = (1 + D)/2 \quad ,$$

$$b_k = (a_k + a_{k-1})/2 \quad ,$$

$$h = 1/2 \quad ,$$

$$\phi(t) = \pi \int_{-\infty}^{t} \sum_{k=-\infty}^{\infty} b_k \, g(t - kT)dt \quad ,$$

and

$$g(t) = \begin{cases} \frac{1}{2T} & 0 \leq t \leq T \\ 0 & \text{elsewhere} \, . \end{cases}$$

From the definition of b_k it can be seen that a phase shift of $\pm \pi/2$ radians occurs in a given bit interval if $a_k = a_{k-1}$, while the phase is constant if $a_k \neq a_{k-1}$.

Due to the partial response encoding of the bits in DMSK it is necessary to define the state of the modulation at the start of each bit interval. The state at $t = kT$ is

given by the pair

$$[\phi(kT),\ \alpha_{k-1}] \quad .$$

The interaction between the various states can be described quite easily using a phasor state diagram. Such a diagram is shown in Fig. 2.6.

Following the technique presented by Galko and Pasupathay [24] it is possible to consider DMSK as MSK with intersymbol interference. The first thing to notice is that in DMSK the phase change due to any a_k is always $\pm \pi/2$ radians; $\pm \pi/4$ radians in the b_k term and $\pm \pi/4$ radians in the b_{k+1} term. Assuming, without loss of generality, that $\phi(0) = 0$

$$\phi(kT) = \frac{\pi}{2} \sum_{i=0}^{k-1} a_i - \frac{\pi}{4} a_{k-1} + \frac{\pi}{4} a_{-1} \quad .$$

The a_{k-1} term is subtracted because it has been implicitly included in the summation. The a_{-1} term is added as it affects the phase in the zeroth interval. The term

$$\frac{\pi}{2} \sum_{i=0}^{k-1} a_i$$

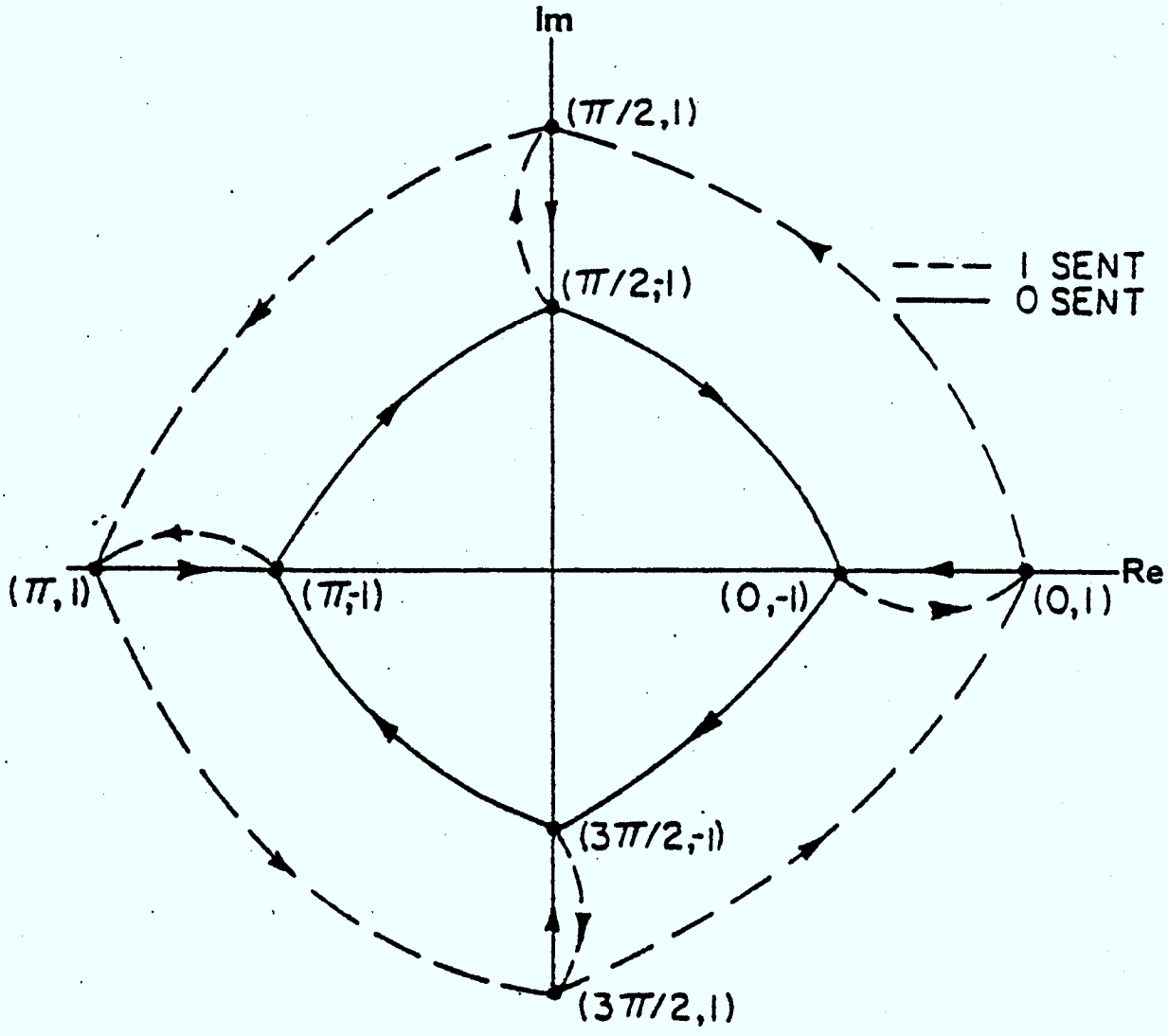

Figure 2.6 : The State Transition Diagram for DMSK

can be recognized as (5), the phase term for MSK. Thus, the term

$$-\frac{\pi}{4} a_{k-1}$$

can be viewed as intersymbol interference and the term

$$\frac{\pi}{4} a_{-1}$$

as a constant phase offset. If the initial phase is set such that

$$\phi(0) = -\frac{\pi}{4} a_{-1} \quad , \tag{6}$$

then

$$\phi(kT) = \frac{\pi}{2} \sum_{i=0}^{k-1} a_i \pm \frac{\pi}{4} \quad . \tag{7}$$

Assuming that the data sequences are identical, and that the initial DMSK phase is as specified, (7) implies that the MSK and DMSK phases will always be within $\pi/4$ radians of each other at $t = kT$. More importantly, the DMSK phase will always be in the same half plane as the MSK phase giving DMSK the half plane property. Thus, DMSK can be

demodulated using a deBuda type receiver as long as the initial phase is chosen as in (6). Again, as in MSK and TFMREC, the source bits must be differentially encoded and a phase error results in a double error in the source bit estimate.

The state of DMSK is restricted to certain values depending upon whether the phase is at the start of an even or odd bit interval. The allowed states are shown in Fig. 2.7 while the phase transitions due to α_k and α_{k+1} are shown in Fig. 2.8.

The I and Q channel waveforms for DMSK should not be sampled at the same time as in MSK. Consider the four possibilities for the DMSK phase at the end of an even bit interval with the initial phase as in (6): if the state is $[\pi/4\ ,\ 1]$ then

$$\phi[(2k+1)T] = \phi_{MSK}[(2k+1)T] - \frac{\pi}{4} \quad ;$$

if the state is $[\pi/4,\ 0]$ then

$$\phi[(2k+1)T] = \phi_{MSK}[(2k+1)T] + \frac{\pi}{4} \quad ;$$

if the state is $[-3\pi/4,\ 1]$ then

$$\phi[(2k+1)T] = \phi_{MSK}[(2k+1)T] - \frac{\pi}{4} \quad ;$$

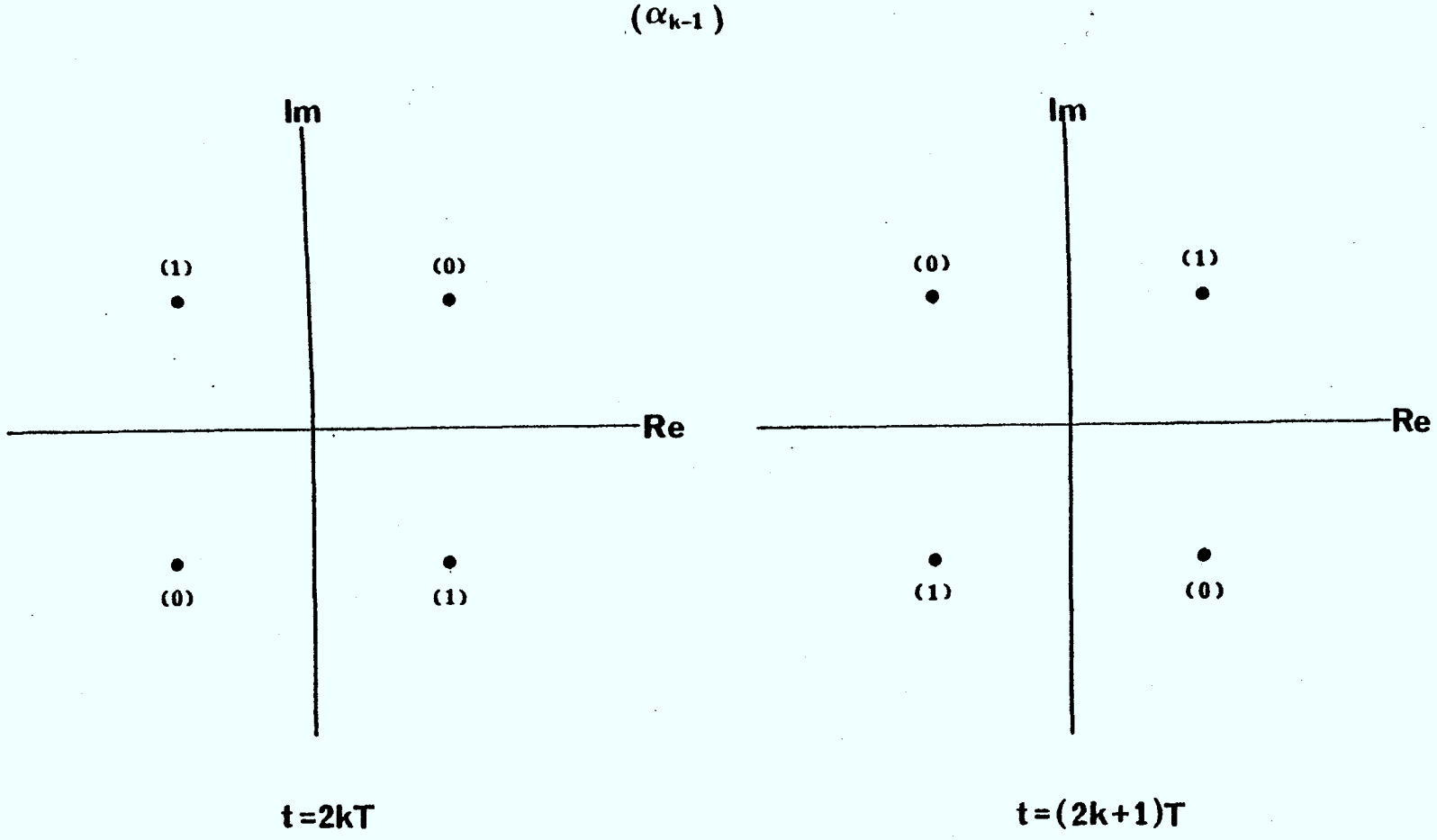

Figure 2.7 : The Allowed States for DMSK with the Half Plane Property of MSK

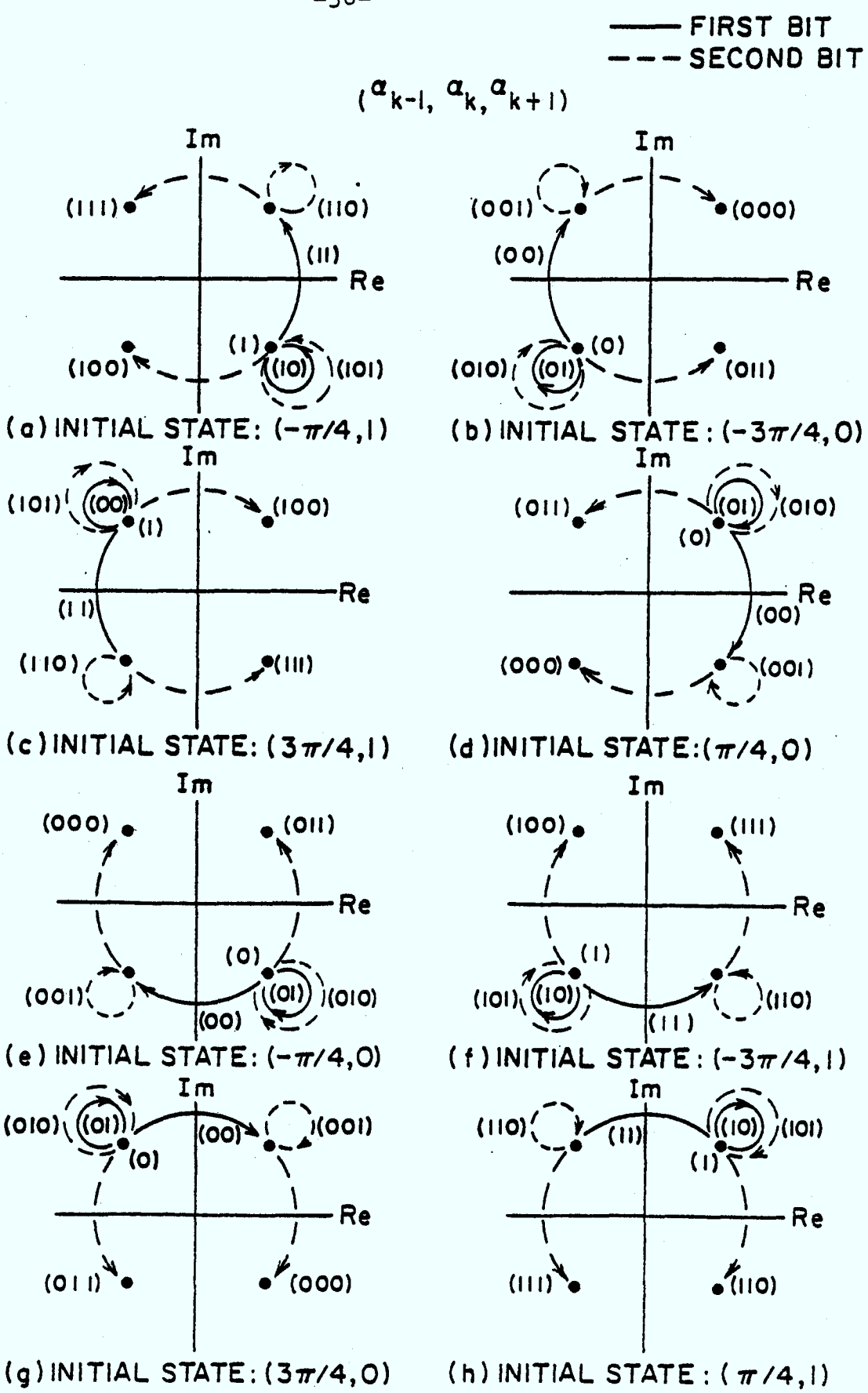

Figure 2.8 : The Phase Transitions for DMSK Over Two Bit Intervals

if the state is $[-\pi/4, 0]$ then

$$\phi[(2k+1)T] = \phi_{MSK}[(2k+1)T] + \frac{\pi}{4} \quad .$$

For MSK the sample in the Q channel takes place at $t = (2k+1)T$ and, assuming no distortion from the receiver filter,

$$r_Q[(2k+1)T] = A \sin[(2n+1)\frac{\pi}{2}] = \pm A \quad ,$$

where $r_Q(t)$ is the signal component in the Q channel after the receive filter and is shown in Fig. 2.3. If the Q channel waveform for DMSK is sampled at the same time then

$$r_Q[(2k+1)T] = A \sin[(2n+1)\frac{\pi}{4}] = \pm \frac{A}{\sqrt{2}}$$

From the above it can be seen that the Q channel waveform should always be sampled at $t = (2k+1 + 1/2)T$. The extra $T/2$ seconds causes the amplitude of the DMSK sample to equal the amplitude of the MSK sample half of the time. The other half of the time the phase is constant in the $(2k+1)^{th}$ bit interval and the delay will not cause a change in the sample amplitude. A similar argument can be made for sampling the

I channel waveform at time $t = (2k+1/2)T$.

DMSK has the property that the phase stays constant in a given bit interval half of the time; this assumes that the source bits are independent. Thus, the pure carrier is transmitted 50% of the time at four different phases. Fourth power carrier recovery techniques can thus be used to extract the carrier reference; however, a 90° ambiguity will result in the phase and the deBuda receiver can only resolve a 180° ambiguity. Using the pure carrier should provide better carrier recovery than that for the deBuda receiver [8] which was designed for MSK. A receiver has been developed for DMSK that resolves a 90° phase ambiguity at the expense of increased sensitivity to noise. This receiver is described below; it is referred to as receiver 2 for DMSK while the deBuda receiver will be referred to as receiver 1.

Receiver 2 for DMSK is shown in Fig. 2.9. For this receiver to work DMSK must be generated with $\phi(0) = n\pi/4$, where n is an odd integer; this means that

$$\phi(kT) \in \{\frac{\pi}{4}, -\frac{\pi}{4}, \frac{3\pi}{4}, -\frac{3\pi}{4}\} .$$

The receiver detects whether or not the phase has changed during a bit interval. The detection is made by observing

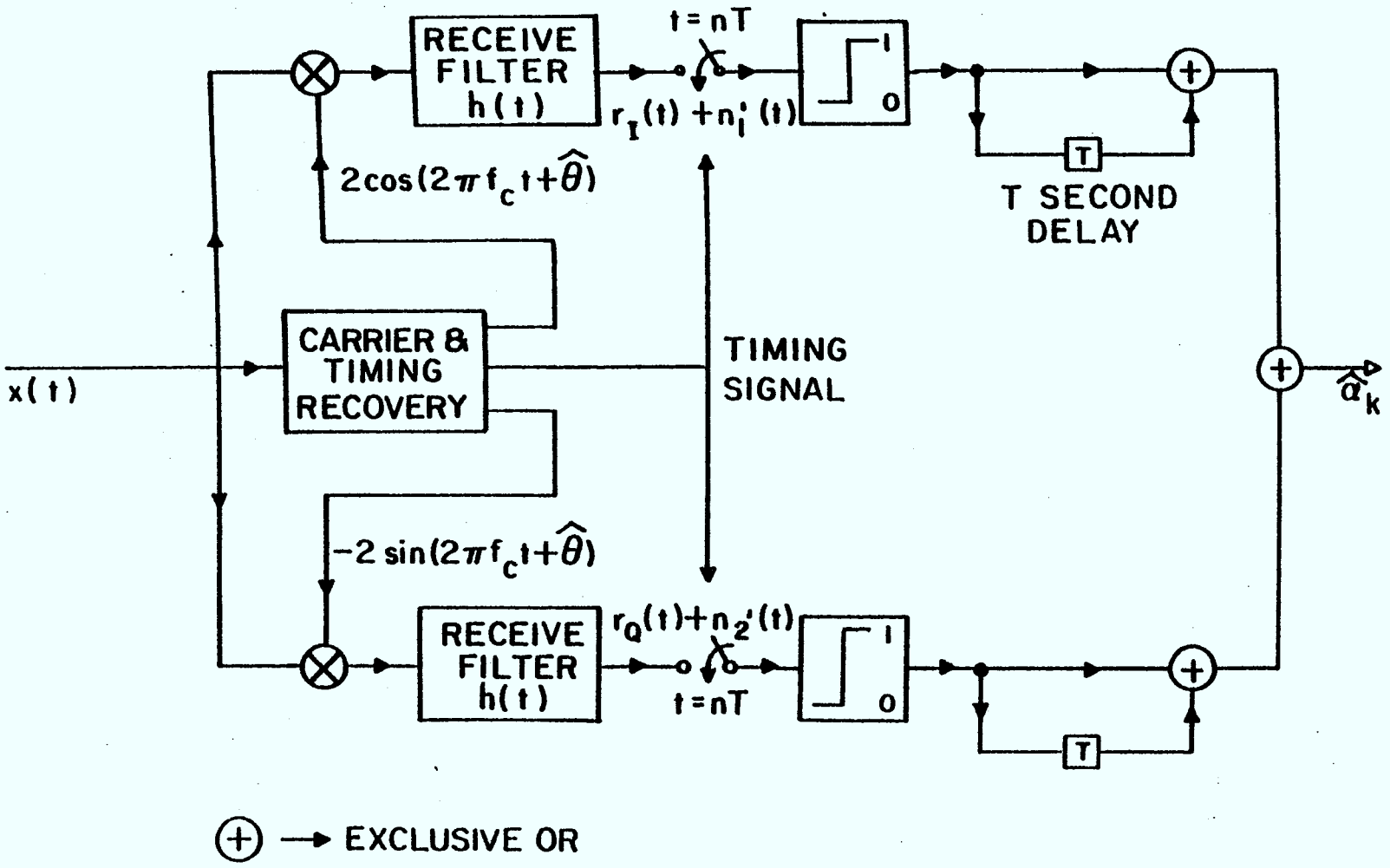

Figure 2.9 : Receiver 2 for DMSK

both the I and Q channels together. If either channel output changes, ignoring noise and distortion, there must have been a phase transition; if neither changes then there was no phase transition. Mathematically,

$$\cos[\phi(kT)] = \cos\{\phi[(k+1)T]\}$$

and

$$\sin[\phi(kT)] = \sin\{\phi[(k+1)T]\}$$

implies that there was no phase transition in the k_{th} bit interval. It is impossible for the samples of both channels to change during one bit interval. Thus, the output of the receiver will be high if a phase transition occurs and low if no phase transition occurs. A phase transition implies that $a_k = a_{k-1}$ while no phase transition implies that $a_k \neq a_{k-1}$. Therefore, it is necessary to use differential encoding of the source bits to get estimates of the source bits at the receiver output. The exclusive OR gates detect transitions in the channels. Due to its memory, this receiver also has the property than an error in detecting a phase transition results in a double error in the estimate

of the source bit stream.

It is possible to detect errors in DMSK by observing patterns of phase changes; the process is similar to that done with patterns of bit changes in ordinary duobinary transmission [7]. In DMSK the polarities of the $\pi/2$ radian phase changes on either side of a consecutive string of no phase changes must be opposite if the number of intervals with no phase change is odd; the polarities must be the same if this number is even. If the above condition is not satisfied than an error must have occurred and retransmission can be requested. Error detection cannot be done in this way with MSK as MSK has no memory. It should be possible to detect errors in TFMREC but the rules are expected to be quite complicated.

An implementation technique for the above error detection technique has been designed for use with receiver 2 for DMSK. This implementation can be adapted for use with receiver 1 by including parts of receiver 2 in receiver 1. The error events can be detected by observing the I and Q channel outputs, after their respective exclusive OR gates, on either side of a string of no phase changes. A no phase change occurs when the output of the receiver is zero. A flip flop can thus be set or cleared depending upon whether the number of no phase changes is even or odd.

Memory elements are used to store the I and Q channel outputs. The set {a,b,c} has the following meaning: a is the channel output two bit intervals before the start of the no phase change string, b is the channel output one bit interval before, and c is the output after the string. It should be noted that the channel output will be b throughout the string of no phase changes. The error events for either channel are shown below as {a,b,c} in Table 2.2.

I or Q Channel	I or Q Channel
{1,1,1}	{1,1,0}
{0,0,0}	{1,0,0}
{1,0,1}	{0,0,1}
{0,1,0}	{0,1,1}
(a) An Even Number of No Phase Changes	(b) An Odd Number of No Phase Changes

Table 2.2: Error Events in the Channels

CHAPTER 3

STANDARD LOW PASS FILTERS AS RECEIVER ARM FILTERS

The receivers in Figures 2.3 and 2.9 are not complete unless the receive filters are specified. For MSK, as in QPSK, the I and Q channel waveforms are made up of one basic pulse shape that is repeated again and again. The optimum arm filter is the one matched to the respective pulse shape. These pulses are: for MSK

$$p(t) = \begin{cases} A \cos\left(\frac{\pi t}{2T}\right) & -T \leq t \leq T \\ 0 & \text{elsewhere} , \end{cases}$$

and for QPSK

$$p(t) = \begin{cases} A/\sqrt{2} & -T \leq t \leq T \\ 0 & \text{elsewhere} . \end{cases}$$

The matched filter error performance in a receiver, without differential encoding, on a white Gaussian noise channel will be [25]

$$P_e = Q\left(\sqrt{\frac{2\ E_b}{N_o}}\right) \quad ,$$

where the Q function is defined as

$$Q(x) = \frac{1}{\sqrt{2\pi}} \int_x^\infty e^{-\nu^2/2}\ d\nu \ .$$

The performance with a maximum likelihood receiver can be upper bounded by [25]

$$Q\left[\sqrt{\frac{E_b\ d^2_{min}}{N_o}}\right] .$$

Thus, from Table 2.1, it is seen that the matched filter receiver and the maximum likelihood receiver perform identically for MSK and QPSK. For most CPM modulations, including DMSK and TFMREC, there is more than one basic pulse shape. This multiplicity of pulse shapes means that there is no matched filter and an alternative must be found for the arm filters. Some strategies to find these filters have been discussed in section 1.3. Many of the filters found

with these strategies are quite complicated and require correlations over many bit intervals. The correlations are usually implemented using weighted integrate and dump circuits; these need the generation of a complex signal, a multiplier, and precise timing of the dump operation. Also, in channels with distortion the best suboptimal filter may have much greater distortion loss than a simpler filter.

It is of interest to consider the use of standard low pass filters as the receive filters. I and Q receivers using these standard filters have a probability of error that is close to the smallest obtainable. Also, the standard filters are much cheaper and easier to implement than the best suboptimal filters.

The same filters are used in both the I and Q channels as the channel waveforms are stochastically identical. Also, the analysis need only be done for one of the two channels.

The performance of the modulations with their receivers is first dealt with assuming no filter distortion. The effects of various standard low pass filters as the receive filters is then considered and the best standard low pass filter found for each modulation.

3.1 The Performance of the Modulations Assuming No Filter Distortion

Assuming without loss of generality that $\phi(0) = 0$ it is found that for MSK

$$\phi(t) = \begin{cases} 0 \ , \ \pi & t = 2kT \\ \frac{\pi}{2} \ , \ \frac{3\pi}{2} & t = (2k+1)T \end{cases} .$$

Therefore, for the receiver in Fig. 2.3

$$r_I(2kT) = A \cos[\phi(2kT)] = \pm A \quad .$$

The expression for the probability of error for MSK can thus be written as

$$P_e = 2\{\tfrac{1}{2} P_r[r_I(2kT) + n_i'(2kT) < 0 \mid \phi(2kT) = 0]$$

$$+ \tfrac{1}{2} P_r[r_I(2kT) + n_i'(2kT) \geq 0 \mid \phi(2kT) = \pi]\}$$

$$= 2Q\left(\frac{A}{\sigma_n'}\right) \quad , \qquad (8)$$

where $n_i'(t)$ is the noise at the receiver filter output, and $\sigma_{n'}^2$ is its variance. The factor of two in the above

expression is due to the error run of length two in the deBuda receiver.

The probability of error of TFMREC in the in phase channel at t = 2kT is the same no matter what the state of the modulation at t = (2k-2)T. The reason for this invariance is that $\cos[\phi(2kT)]$ always equals one of the set $\{1, -1, 1/\sqrt{2}, -1/\sqrt{2}\}$ each with equal probability. For example, assume that at t = (2k-2)T the TFMREC state is given by [0,1,1]. Then, at t = 2kT the possible phases are: 0, $\pi/4$, $3\pi/4$, π. Similar reasoning can be made for the quadrature channel. The probability of error can be found by finding it for any one of the eight possible states at t = (2k-2)T. Assuming the state to be [0,1,1] it is found that

$$P_e = 2\{\tfrac{1}{4} P_r[r_I(2kT) + n_1'(2kT) < 0 \mid \phi(2kT) = 0]$$

$$+ \tfrac{1}{4} P_r[r_I(2kT) + n_1'(2kT) < 0 \mid \phi(2kT) = \pi/4]$$

$$+ \tfrac{1}{4} P_r[r_I(2kT) + n_1'(2kT) > 0 \mid \phi(2kT) = 3\pi/4]$$

$$+ \tfrac{1}{4} P_r[r_I(2kT) + n_1'(2kT) > 0 \mid \phi(2kT) = \pi]\}$$

$$= Q\left(\frac{A}{\sigma_{n'}}\right) + Q\left(\frac{A}{\sqrt{2}\sigma_{n'}}\right) \quad . \tag{9}$$

The factor of two in front of the brackets

is due to the receiver's double error property.

Recall that in DMSK with the deBuda type receiver the I channel waveform is sampled at $t = (2k+\frac{1}{2})T$ and the Q channel waveform at $t = (2k+1+\frac{1}{2})T$. Using the I channel and examining Figures 2.6 and 2.7 it can be seen that no matter what the state at $t = 2(k-1)T$ the term $\cos\{[(2k+\frac{1}{2})T]\}$ will always be from the set $\{1, -1, 1/\sqrt{2}, -1/\sqrt{2}\}$; each of the elements occurring with equal probability. For example, if the state at $t = 2(k-1)T$ is $[\pi/4, 0]$ then

$$\phi[(2k+\tfrac{1}{2})T] \in \{\tfrac{3\pi}{4}, \pi, \tfrac{-3\pi}{4}, 0, \tfrac{\pi}{4}, \tfrac{-\pi}{4}\}$$

with 0 and π having twice the probability of the others. Thus, $\cos\{[\phi(2k+\frac{1}{2})T\}$ is from the same set as $\cos[\phi(2kT)]$ in TFMREC and the performance of DMSK with receiver 1 will be the same as that of TFMREC.

When using receiver 2 for DMSK both of the channels must be considered together as an error in either channel will result in a decision error. The probability of error at $t = kT$ is independent of the state at $t = (k-1)T$. The probability of error in each channel is also assumed to be independent of the probability of error in the other channel. Also, the probability of getting an error in

both channels at once is very small and can be ignored. Assume that the state at $t = (k-1)T$ is $[\pi/4, 1]$, then

$$P_e = 2\{\tfrac{1}{2} P_r[r_I(kT) + n_1'(kT) \gtrless 0 \mid \phi(kT) = \tfrac{3\pi}{4}]$$

$$+ \tfrac{1}{2} P_r[r_Q(kT) + n_2'(kT) < 0 \mid \phi(kT) = \tfrac{3\pi}{4}]$$

$$+ \tfrac{1}{2} P_r[r_I(kT) + n_1'(kT) < 0 \mid \phi(kT) = \tfrac{\pi}{4}]$$

$$+ \tfrac{1}{2} P_r[r_Q(kT) + n_2'(kT) < 0 \mid \phi(kT) = \tfrac{\pi}{4}]\}$$

$$= 4\, Q\left(\frac{A}{\sqrt{2}\,\sigma_{n'}}\right). \qquad (10)$$

Again, the factor of 2 is due to the error run property of the receiver.

The probability of error expressions in (8), (9), and (10) are plotted against A^2/σ_n^2, in Fig. 3.1. It is seen that the performance of MSK is 3 dB better than that of DMSK with receiver 2. The performance of TFMREC and DMSK with receiver 1 tend to that of DMSK with receiver 2 as A^2/σ_n^2, gets large.

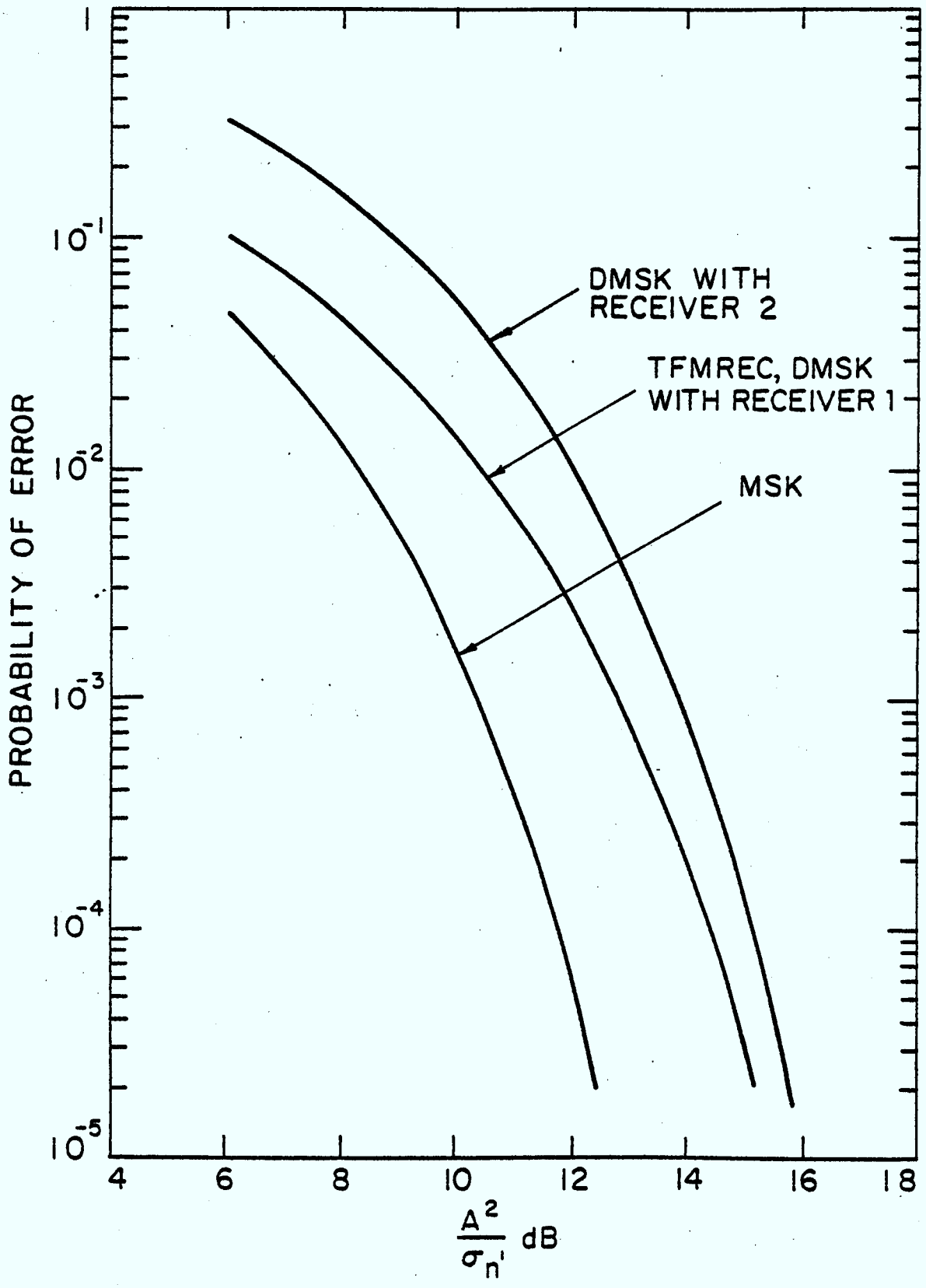

Figure 3.1 : The Probability of Error for MSK, TFMREC, and DMSK Assuming No Filter Distortion

3.2 The Method for Calculating the Performance

Due to the correlative encoding and the non-linearity of the modulation it is difficult to calculate the effects of the receive filter on $r_I(t)$ and $r_Q(t)$ analytically. Also, the non-linearity makes it impossible to use a bound for the amount of intersymbol interference such as that developed by Glave [26].

It is possible to find the probability of error numerically if the intersymbol interference is assumed to extend over a finite amount of time. Mathematically,

$$p_i(t) * h(t) = 0 \quad LT < t < 0$$

where $p_i(t)$ is the ith basic pulse shape for the modulation, $h(t)$ is the impulse response of the receiver arm filter, * denotes convolution, and L is an integer. The receive filter is assumed to be causal.

It is of interest to consider the noise component after the receive filters. The noise will still be Gaussian as the filters are linear [25]; however, the power spectrum will no longer be flat. The autocorrelation function , $R_{n_1}'(\tau)$ and $R_{n_2}'(\tau)$, of the noise after

the filters is given by [25]

$$R_{n_1}'(\tau) = R_{n_2}'(\tau) = \int_{-\infty}^{\infty} S_{n_1}'(f) e^{j2\pi f\tau} df$$

where $S_{n_1}'(f)$ is the power spectrum of the noise at the filter output. If $S_{n_1}(f)$ is the power spectrum of the noise before the filter then

$$S_{n_1}'(f) = |H(f)|^2 S_{n_1}(f)$$

where H(f) is the Fourier transform of h(t). As $S_{n_1}(f) = N_o$ for all frequencies where the magnitude of $|H(f)|^2$ is significant

$$R_{n_1}'(\tau) = R_{n_2}'(\tau) = N_o \int_{-\infty}^{\infty} |H(f)|^2 e^{j2\pi f\tau} df \quad . \qquad (11)$$

This autocorrelation function is plotted in Fig. 3.2 for some of the receive filters that were used in this thesis. The sampling points are spaced 2T seconds apart for the deBuda receiver and T seconds apart for receiver 2 for DMSK. From Fig. 3.2 it is seen that the autocorrelation function for $\tau = 2T$ is quite small, and for $\tau = 2kT$, $k = 2,4,\ldots$, it is very close to zero. The correlation of the noise is significant at $\tau = T$ for the

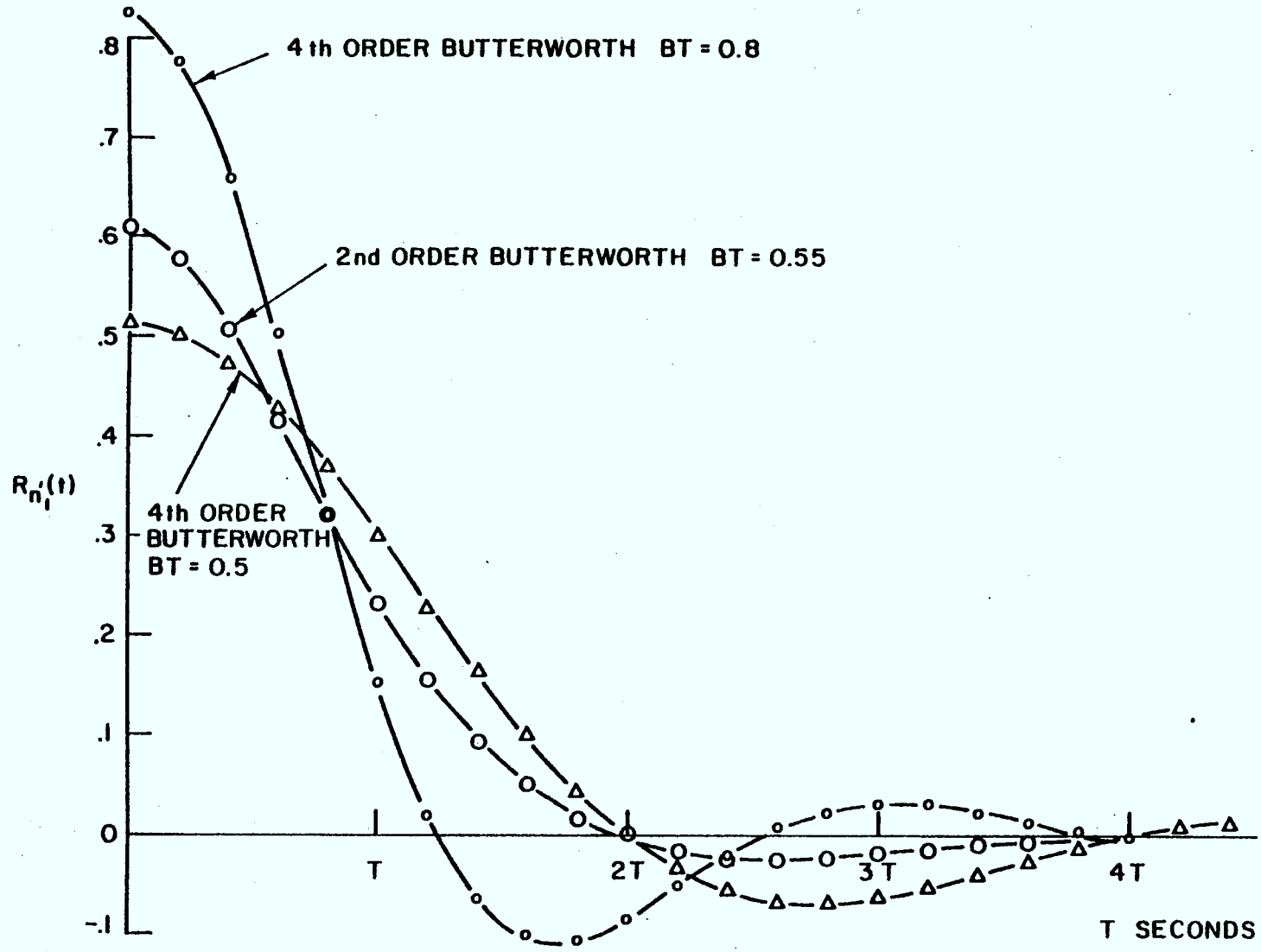

Figure 3.2 : The Autocorrelation of the Noise

filters with the smaller BT products. However, the filters with the larger BT products, around BT = 0.8, are the ones that are used with receiver 2 for DMSK. Thus, it is reasonable to assume that the noise samples are uncorrelated. This assumption makes it much easier to calculate the probability that an entire block of bits are correct.

In order to find the expected value of the probability of error in the k_{th} bit interval, all possible waveforms that can exist in the block of bit intervals that affect the sample must be considered. Assuming that the ISI is smaller than the sample at $t = t_k$ minus the ISI, the probability of error for the i_{th} waveform can be written as

$$P_{e_i} = 2P_r[|r_i(t_k + \gamma)| + n_i'(t_k + \gamma) < 0]$$

$$= 2Q\left[\frac{|r_i(t_k + \gamma)|}{\sigma_n'}\right] ,$$

where $r_i(t)$ is the output of the receive filter for the i_{th} waveform, t_k is the sampling point for this waveform in the k_{th} bit interval, assuming no filter delay or distortion, and γ is a sampling offset due to delay and distortion in the receive filter. It should be noted that if the delay is such that $\gamma + t_k > nT$, where n is a positive integer greater than k, then

the input to the filter for the n - k bit intervals following the k_{th} bit interval will also affect $r_i(t_k + \gamma)$. Thus, it would seem that each waveform should consist of L + ℓ bit intervals where

$$\ell = \max\ n - k : \gamma + t_k > nT \quad .$$

However, only the L - 1 - ℓ bits prior to the k_{th} bit will affect the sample. From symmetry considerations, it can be seen that both $r_i(t)$ and $-r_i(t)$ must be members of the set of possible waveforms. As all waveforms are equiprobable, and as the waveforms $r_i(t)$ and $-r_i(t)$ will have the same error probability, the one whose sample, before the filter, at $t = t_k$ is negative can be dropped from the set of waveforms of interest. The number of waveforms of interest is thus

$$N = m\ 2^{L-1}$$

where m is the number of possible states at time $t = (k - L + 1 + \ell)T$. The expected value of the probability of error can be found by taking the average over the error probabilities of all of the waveforms of interest.

$$E[P_e] = \frac{1}{N} \sum_{i=1}^{N} 2Q \left[\frac{r_i(t_k + \gamma)}{\sigma_{n'}} \right]$$

where $E(\cdot)$ denotes the expectation operation. From [25] it is known that

$$\sigma_{n'}^2 = R_n'(0) \quad .$$

Thus, from (11)

$$\sigma_{n'}^2 = N_o \int_{-\infty}^{\infty} |H(f)|^2 df \quad .$$

Also, for CPM modulations

$$E_b = \frac{A^2 T}{2} \quad .$$

Thus,

$$E[P_e] = \frac{2}{N} \sum_{i=1}^{N} Q \left[r_i(t_k + \gamma) \sqrt{\frac{2E_b}{A^2 T N_o \int_{-\infty}^{\infty} |H(f)|^2 df}} \right] . \qquad (12)$$

In order to calculate the sample values the waveforms

for the in phase channel are considered,

$$r_i(t) = \begin{cases} A \cos[\phi_i(t)] * h(t) & (k-L+1+\ell)T < t < (k+\ell+1)T \\ 0 & \text{elsewhere} \end{cases}$$

$$= u_i(t) * h(t)$$

where $\phi_i(t)$ is the phase for the i_{th} waveform. It is possible to divide each of the N different waveforms, $u_i(t)$, up into L constituent parts each of length T seconds. Thus, the value of the sample for the k_{th} bit can be calculated as below.

$$r_i(t) = \int_{-\infty}^{\infty} u_i(\tau)\, h(t - \tau(d\tau)$$

$$= \int_{(k-L+1+\ell)T}^{(k-L+2+\ell)T} u_i(\tau)\, h(t - \tau)d\tau + \int_{(k-L+2+\ell)T}^{(k-L+3+\ell)T} u_i(\tau)\, h(t - \tau)d\tau$$

$$+ \ldots + \int_{(k+\ell)T}^{(k+\ell+1)T} u_i(\tau)\, h(t - \tau)d\tau \quad . \qquad (13)$$

For any of the CPM modulations each $u_i(t)$ is composed of a finite number, M, of T length pulses. These pulses

are: $p_1(t)$, $p_2(t)$, $p_3(t)$,..., $p_M(t)$; also,

$$p_j(t) = 0 \qquad T < t \leqslant 0 \qquad j = 1,2,\ldots, M \ .$$

The actual number and shape of the pulses is determined by the modulation scheme. Thus, (13) can be rewritten as

$$r_i(t) = \int_{-\infty}^{\infty} p_j^1[t - (k - L + 1 + \ell)T]\, h(t - \tau)d\tau$$

$$+ \int_{-\infty}^{\infty} p_j^2[t - (k - L + 2 + \ell)T]\, h(t - \tau)d\tau$$

$$+ \ldots + \int_{-\infty}^{\infty} p_j^L[t - (k + \ell)T]\, h(t - \tau)d\tau$$

where

$$p_j^y \ \varepsilon \ \{p_1(t),\ p_2(t),\ldots,\ p_M(t)\} \ .$$

Using the time shift property of the Fourier transform [10],

$$r_i(t) = F^{-1}[e^{j(k-L+1+\ell)T} P_j^1(f)H(f) + e^{j(k-L+2+\ell)T} P_j^2(f)H(f)$$

$$+ \ldots + e^{j(k+\ell)T} P_j^L(f)H(f)] \qquad (14)$$

where F^{-1} denotes the inverse Fourier transform, and $P_j^y(f)$ is the Fourier transform of $p_j^y(t)$.

Using (14) it is seen that to calculate $r_i(t)$ it is necessary only to calculate the response of the filter to each of the M possible pulses. These responses are then shifted in time by the amount shown in the appropriate exponential in (14), and then added together to form the composite waveform, $r_i(t)$. The expected value of the probability of error in (12) can then be calculated.

Due to their different frequency contents, the receive filter distorts each of the possible pulse shapes differently; there is distortion because the phase responses of the receiver filters are, in general, non-linear. This differing distortion makes it difficult to determine Υ, the optimum sampling offset, analytically. At large signal to noise ratios the expected value of the probability of error will be dominated by the worst case $r_i(t_k + \Upsilon)$; this is due to the exponential decrease of $Q(x)$ as x increases.

Thus, a good estimate of the optimum sampling point can be obtained by finding the γ which maximizes the smallest $r_i(t_k + \gamma)$. Mathematically, the metric J is evaluated and the appropriate γ chosen where

$$J = \max_{\gamma} \min_{i} r_i(t_k + \gamma).$$

The truly optimum γ will be a function of the signal to noise ratio (SNR) as the importance of each term in (12) changes with the SNR.

3.2 Results Using the Standard Low Pass Filters

The receivers for MSK, QPSK, TFMREC, and MSK were studied using standard low pass filters as the receive filters. A standard I and Q receiver [6] with differential encoding of the source bits was used for QPSK. Second order Butterworth filters for QPSK receivers have been studied previously [6]; QPSK is used here for comparison purposes. The standard low pass filters used were: second order Butterworth filters, fourth order Butterworth filters, fourth order Chebychev filters with 0.1 dB ripple, and sixth order Butterworth filters. The transfer functions for these filters can be found in

Johnson [27].

The pulse shapes, $p_i(t)$, must be found for each of the modulations. The pulse shapes for MSK and QPSK were given earlier in this chapter; however, these pulses are of length 2T. All of the possible waveforms, $u_i(t)$, over a 2T second interval are shown in Figures 3.3 and 3.4 respectively. From these figures it is possible to identify fourteen different characteristic pulse shapes for TFMREC, while six are possible for DMSK. However, half of these pulses are redundant if the sign of the pulse is ignored. The number of pulse shapes for TFMREC and DMSK for which the filter output must be calculated is thus reduced by a factor of two.

The Fast Fourier Transform (FFT) algorithm [28] was used to compute the discrete Fourier transforms of the pulses; these were then multiplied by the discrete Fourier transform of the appropriate filter to obtain the terms in (14). The inverse discrete Fourier transform was then computed, also using the FFT algorithm, to find the time domain representation of the filtered pulses. The parameters used for the FFT were: 4096 samples, $\Delta t = T/64$ seconds/sample, $\Delta w = \pi/32T$ radians/second.

It was found that the filter response to each pulse

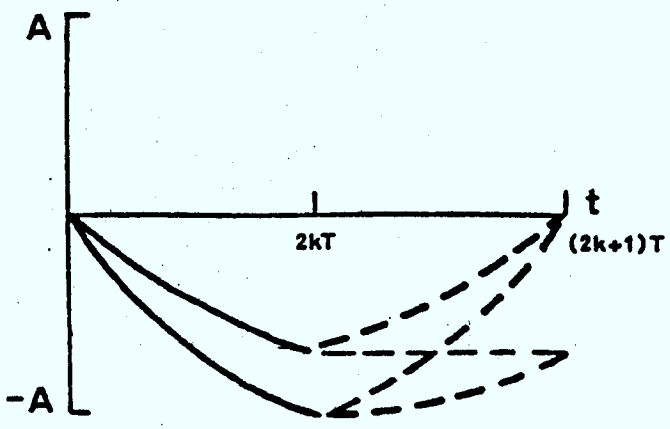

(a) States at t = (2k-1)T
$[\frac{\pi}{2},1,1]$, $[\frac{-\pi}{2},0,0]$

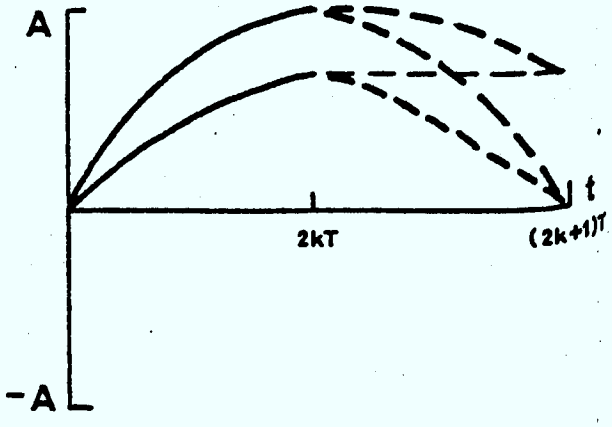

(b) States at t = (2k-1)T
$[\frac{\pi}{2},0,0]$, $[\frac{-\pi}{2},1,1]$

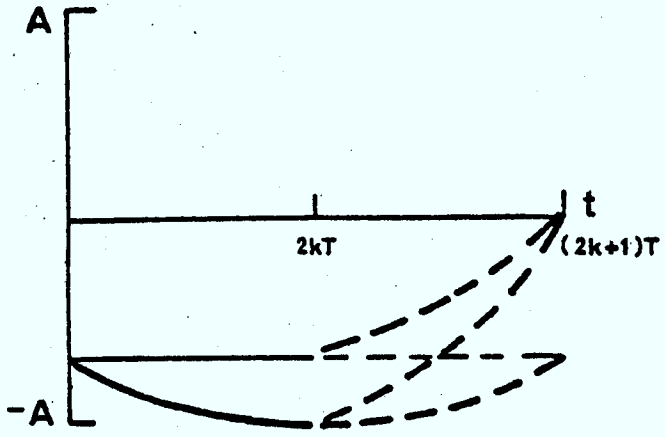

(c) States at t = (2k-1)T
$[\frac{3\pi}{4},0,1]$, $[\frac{-3\pi}{4},1,0]$

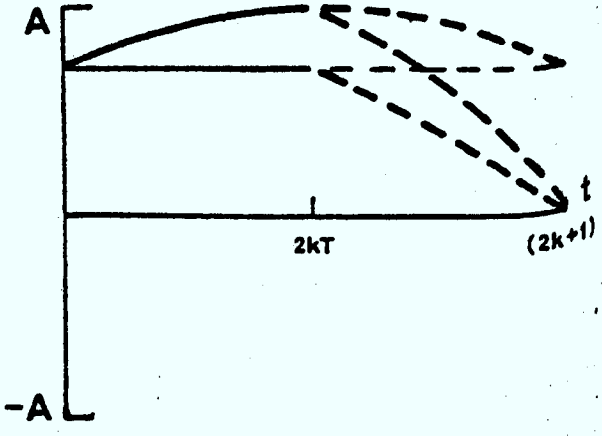

(d) States at t = (2k-1)T
$[\frac{\pi}{4},1,0]$, $[\frac{-\pi}{4},0,1]$

Figure 3.4 : Received Signal Waveforms for TFMREC

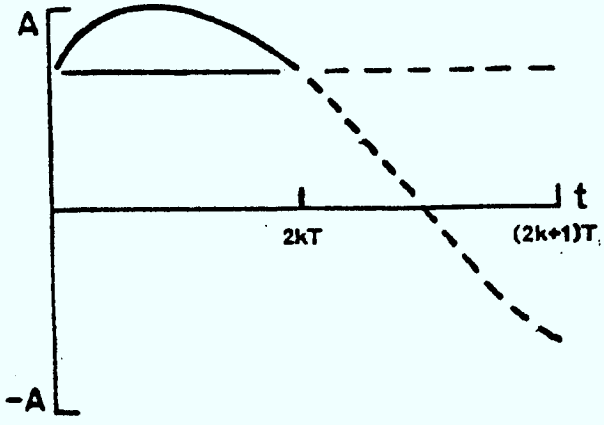

(a) States at t = (2k-1)T
$[\frac{\pi}{4},0]$, $[\frac{-\pi}{4},1]$

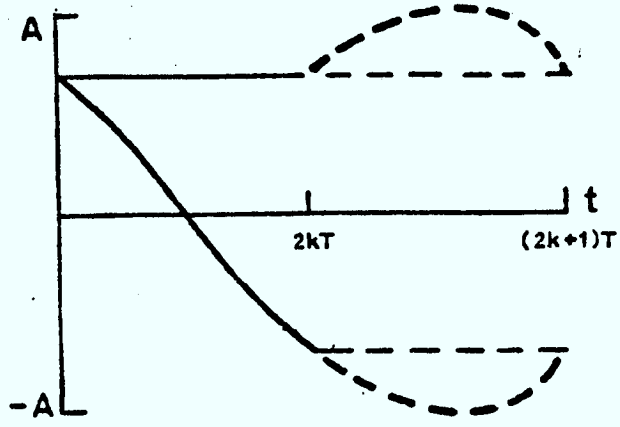

(b) States at t = (2k-1)T
$[\frac{-\pi}{4},0]$, $[\frac{\pi}{4},1]$

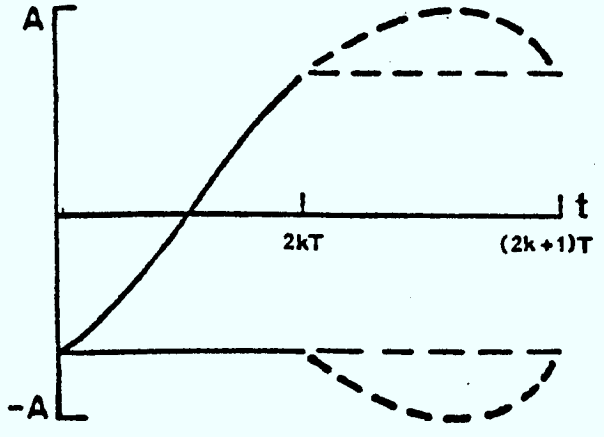

(c) States at t = (2k-1)T
$[\frac{3\pi}{4}, 0]$, $[\frac{-3\pi}{4}]$

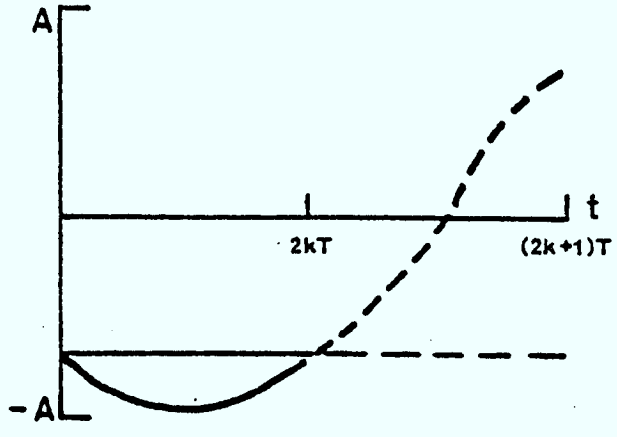

(d) States at t = (2k-1)T
$[\frac{-3\pi}{4},0]$, $[\frac{3\pi}{4},1]$

Figure 3.3 : Received Signal Waveforms for DMSK

was negligible after 11T seconds, and thus the value 11 was assigned to L. It was also found that for all of the filters used $\ell < 4$. Smaller values can be used for L and ℓ with the larger bandwidth filters; the time response dies out faster and there is less delay than with the smaller bandwidth filters.

The optimum standard filter type, and its corresponding best 3 dB bandwidth, B, was found for each of the modulations. This bandwidth was found to increase slightly with the SNR. The probability of error for E_b/N_o = 12 dB has been plotted against the BT product of the receive filter for each filter type in Figures 3.5 to 3.8.* The best bandwidth at E_b/N_o = 12 dB is a reasonable bandwidth to use at all signal to noise ratios. The curves are seen to get more complicated as the frequency cut-off of the filter type becomes sharper; this is due to the phase response of the filters which is more non-linear for the filters with sharper cut-off. Some of the minor aberrations in the curves are due to the suboptimal choice of γ; these disappear at large signal to noise ratios. The results found for QPSK with a second order Butterworth filter were found to be very close to those found by Jones [6] with the same filter type.

---

*Each point on the curves requires about 8 minutes of computation on the VAX-750.

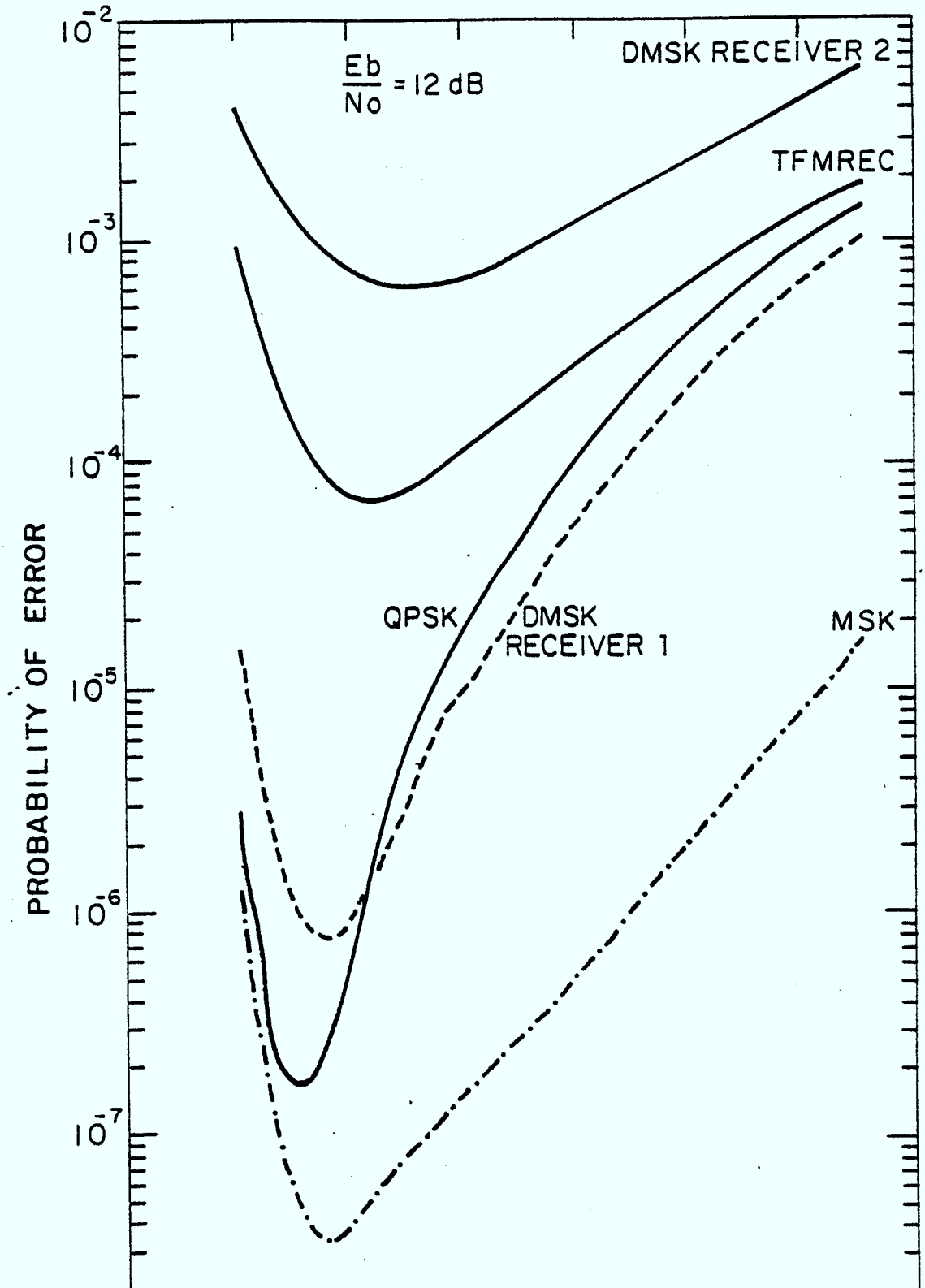

Figure 3.5 : The Receive Filter as a 2nd Order Butterworth Filter - $\frac{E_b}{N_o}$ = 12 dB

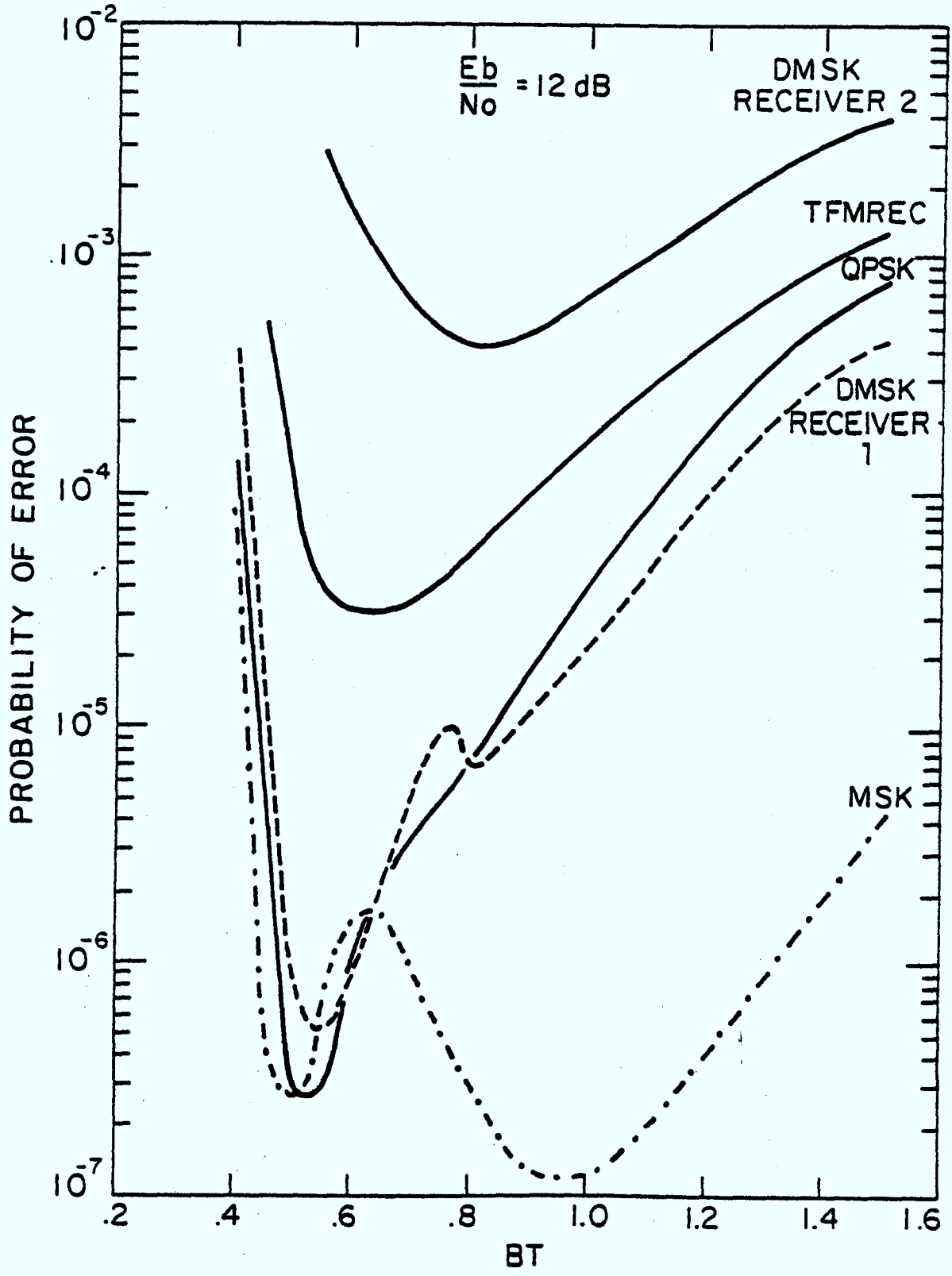

Figure 3.6 : The Receive Filter as a 4th Order Butterworth Filter - $\frac{E_b}{N_o}$ = 12 dB.

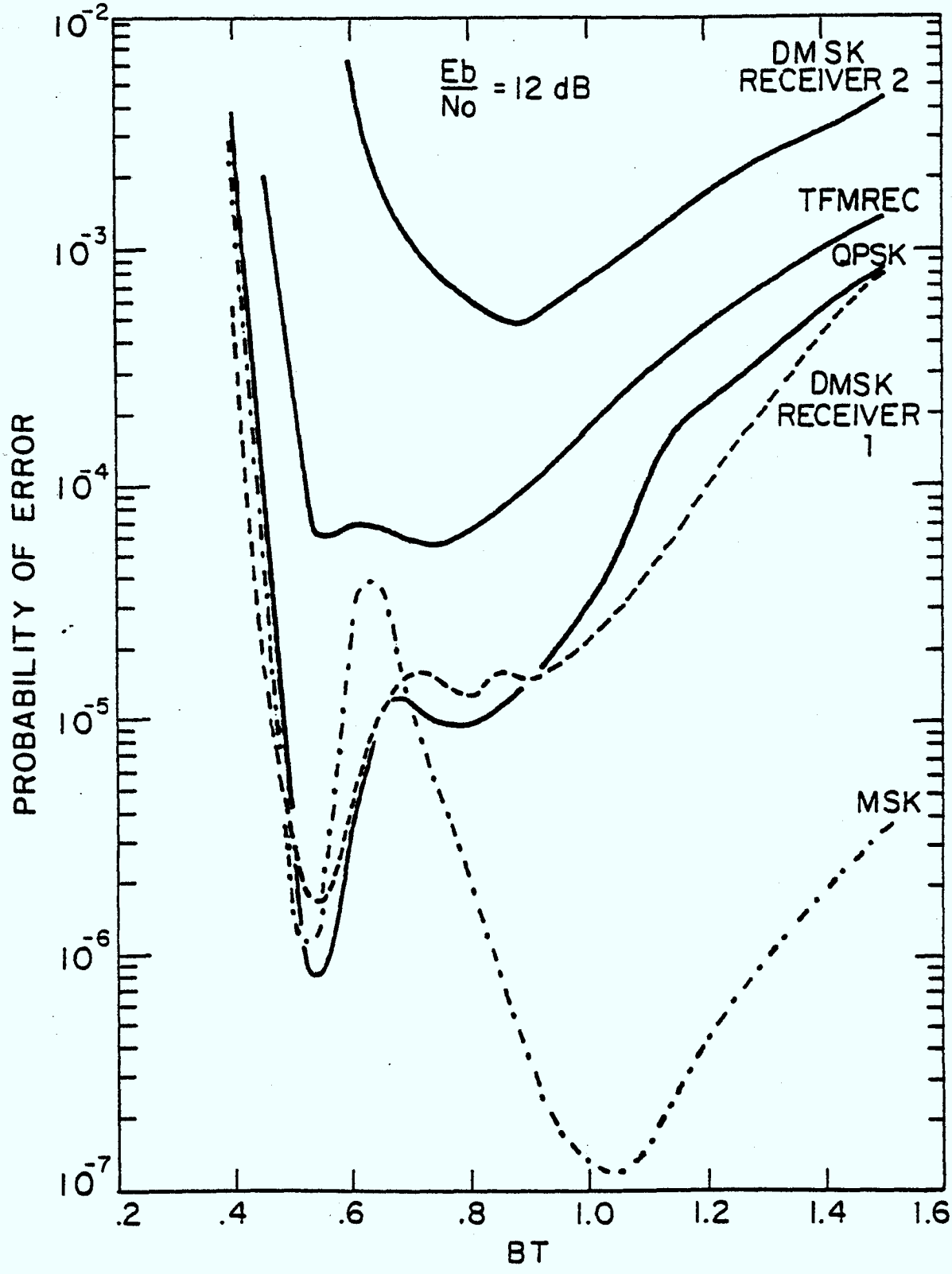

Figure 3.7 : The Receive Filter as a 4th Order Chebychev Filter with ε = 0.1 dB - $\frac{E_b}{N_o}$ = 12 dB

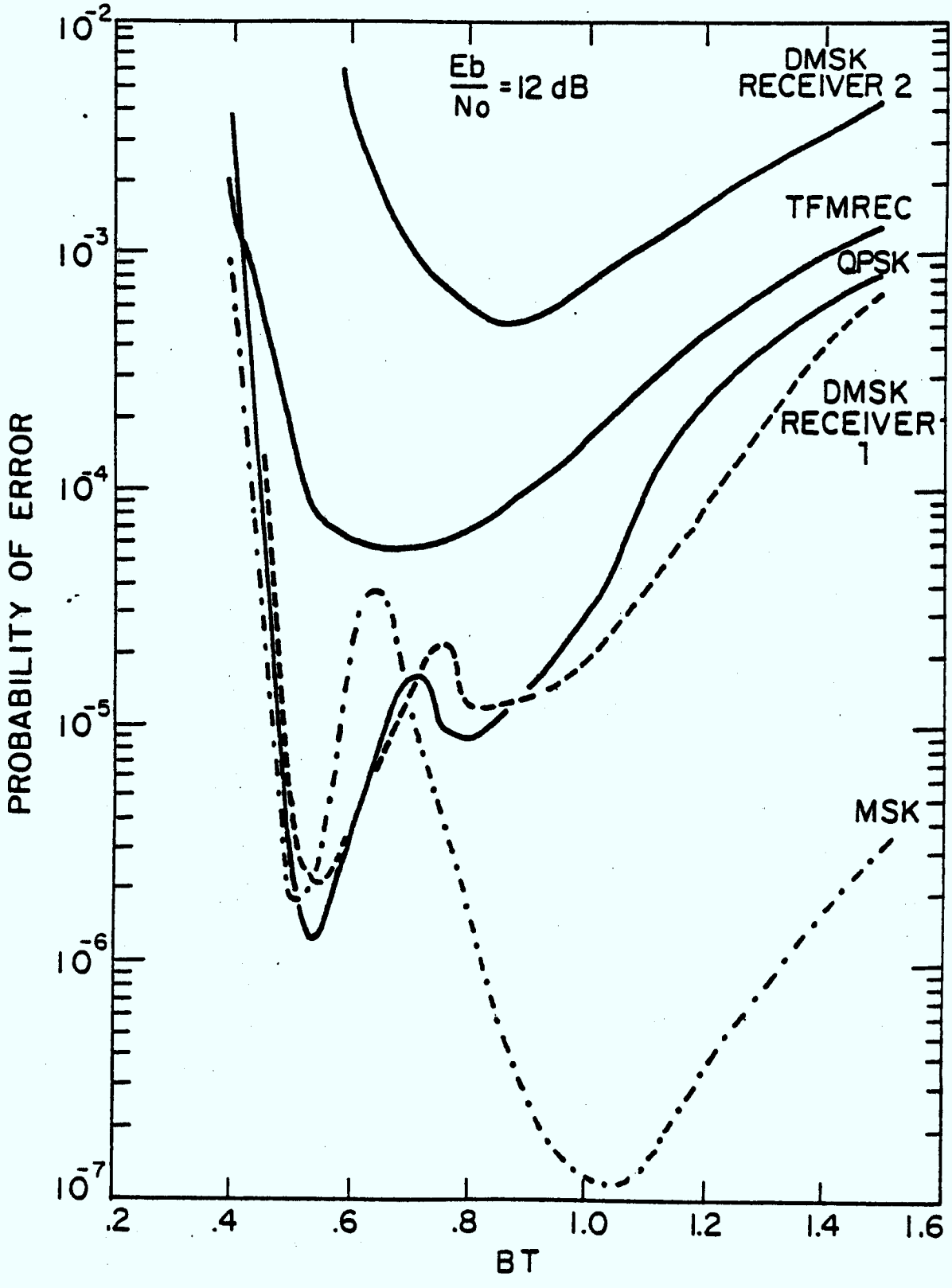

Figure 3.8 : The Receive Filter as a 6th Order Butterworth Filter - $\frac{E_b}{N_o}$ = 12 dB

In a rough sense the best standard low pass filter for each modulation is an approximation to the optimum filter for that modulation; however, due to non-linearities this relationship is not a simple one. In fact, for the general CPM modulation the optimum filter may vary with the signal to noise ratio.

A correspondence between the best standard low pass filter and the optimum filter can be used to explain some of the results. The Butterworth filter is superior to the Chebychev filter because its phase is closer to being linear and its magnitude is maximally flat in the passband. These properties should allow the Butterworth filter to more closely resemble the optimum filter. In modulations with only one basic pulse shape the receive filter is matched to that pulse shape, which lasts for a duration equal to the time between samples. The performance of these modulations thus depends on the energy in the waveform between sample times; this relationship should also exist for modulations with more than one basic pulse shape. Thus, since receiver 2 for DMSK takes samples twice as often as receiver 1 for DMSK, giving it half the energy between samples, it is expected that DMSK will perform approximately 3 dB worse with receiver 1 than with receiver 2. DMSK with receiver 1

is expected to perform better than TFMREC as both waveforms are sampled at 2T second intervals but DMSK has a larger normalized Euclidean distance. The probability of error is plotted against the SNR for each modulation in Figures 3.9 to 3.11. The best standard low pass filter is used for each modulation.

When examining Figures 3.9 to 3.11 it should be remembered that differential encoding of the source bits has been taken into account when calculating the probability of error for the receivers in this thesis; this results in an additional factor of two in the probability of error expression. The results in these figures from other papers have not had differential encoding taken into account. Both the MSK receiver and DMSK with receiver 1 came quite close to the optimal performance with their best standard low pass filters; QPSK and TFMREC both had performances slightly farther from the optimum. The optimum filter for MSK and QPSK is the matched filter, while for DMSK and TFMREC optimal performance is obtained only with a maximum likelihood receiver. The performance of MSK was about 0.5 dB worse than the matched filter bound for the signal to noise ratios in Fig. 3.9; however, the asymptotic performance, obtained with the minimum sample amplitude

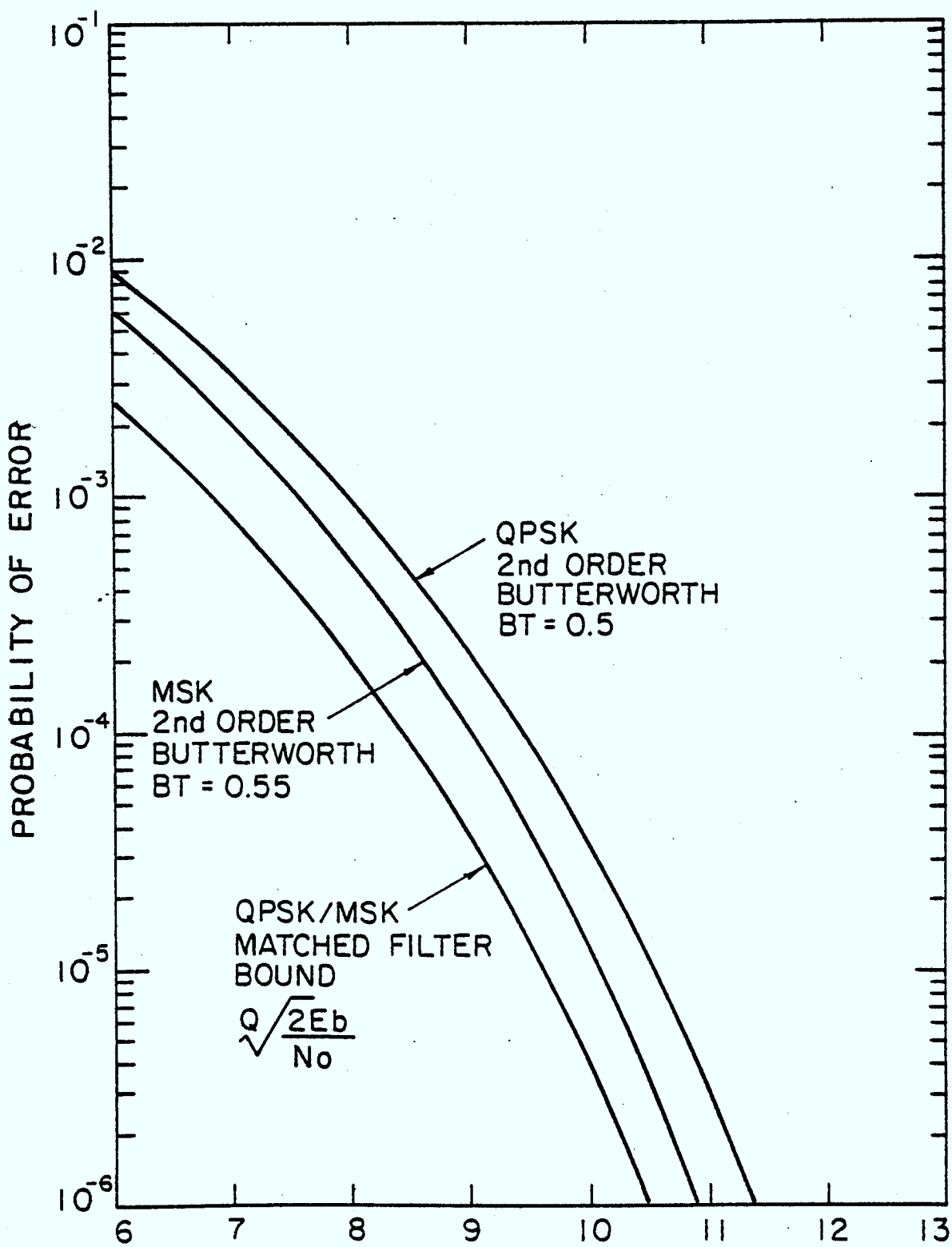

Figure 3.9 : The Performance of MSK and QPSK

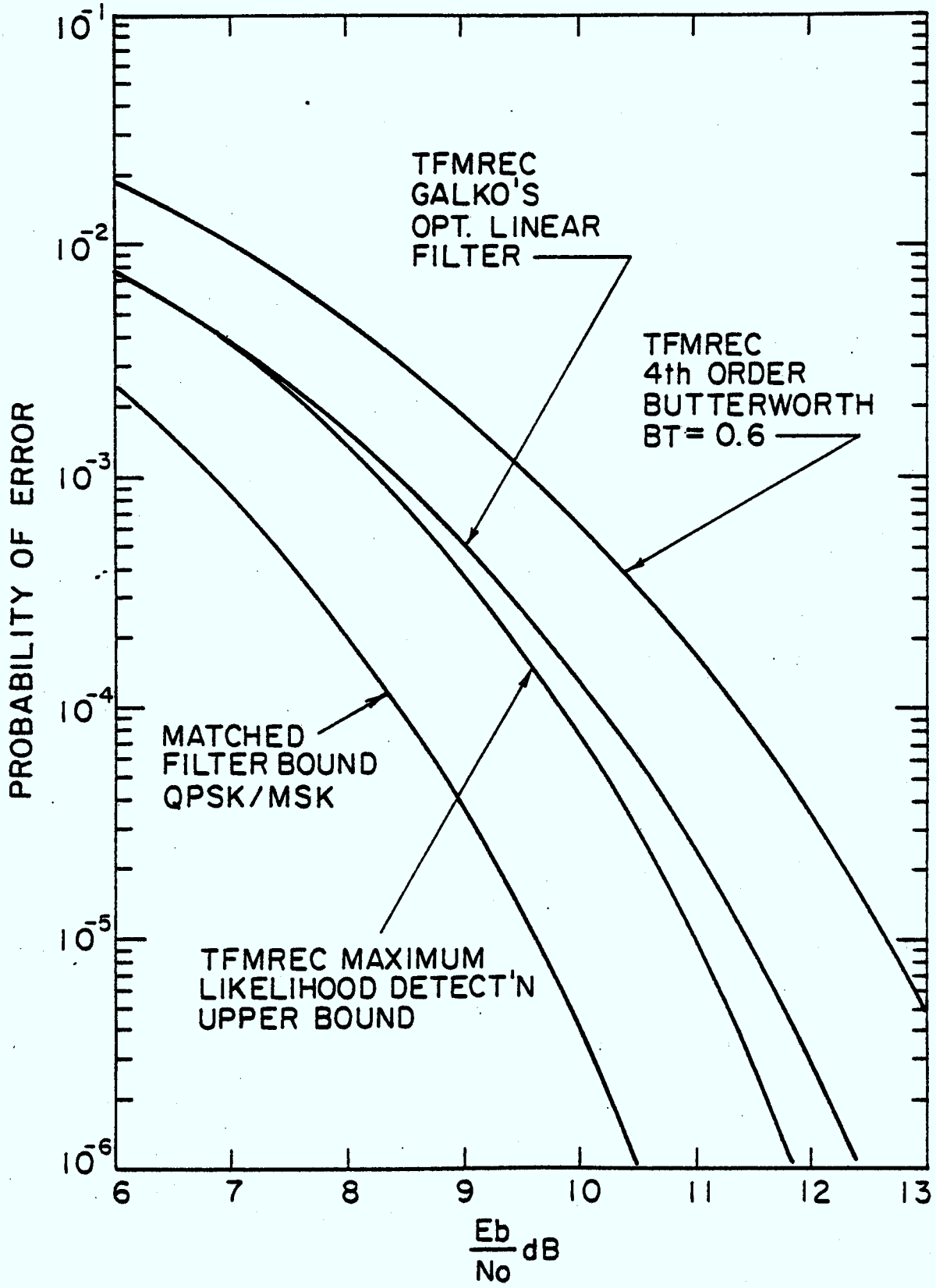

Figure 3.10 : The Performance of TFMREC

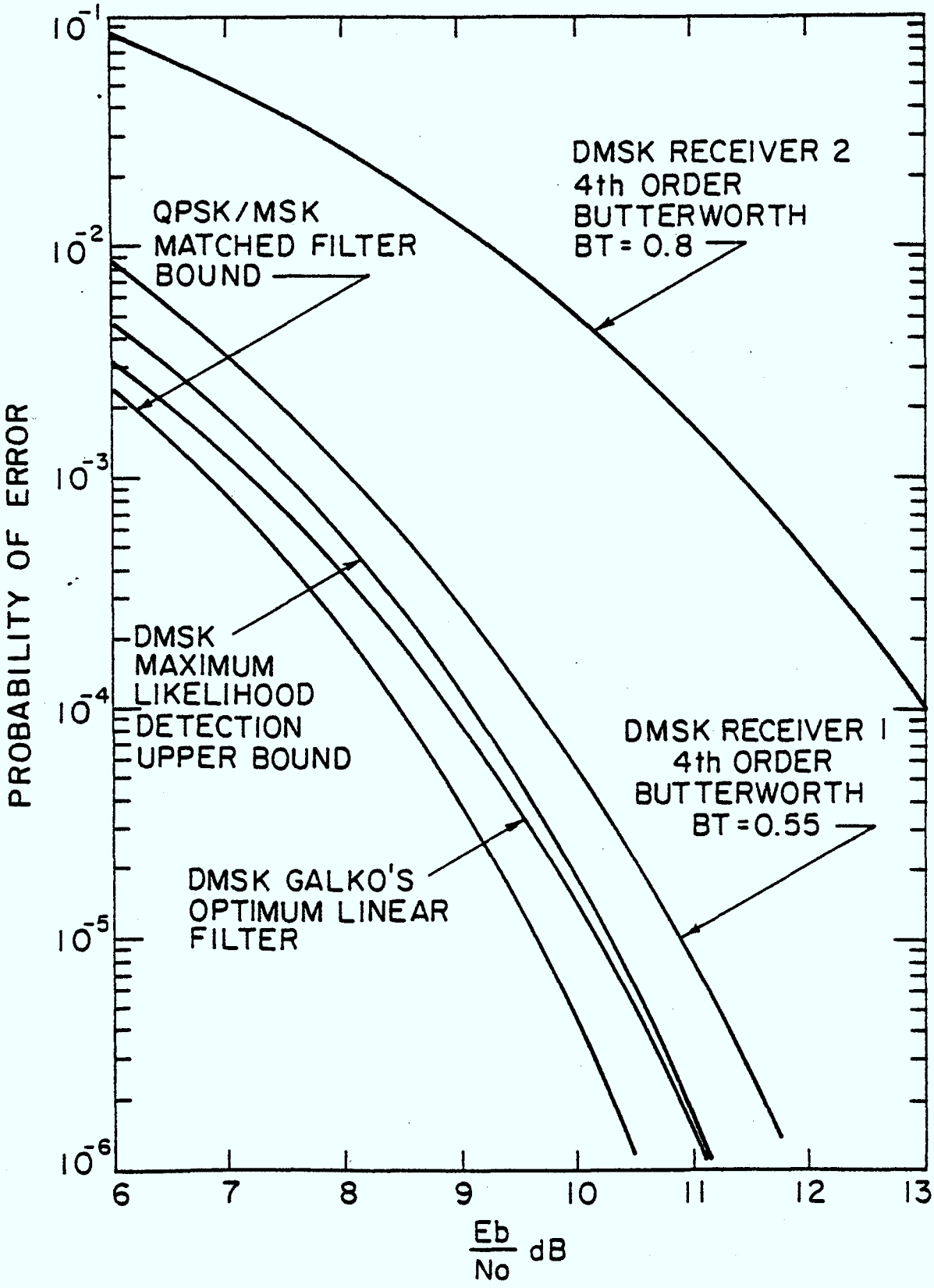

Figure 3.11 : The Performance of DMSK

and ignoring the differential encoding doubling of the error rate, was 0.262 dB worse. When compared with Galko's optimal linear filters [17] it is seen that DMSK, with receiver 1 and standard filters, gives results 0.7 dB worse at $P_e = 10^{-5}$; TFMREC gives results 1.6 dB worse at the same P_e. These differences can be shaded if differential encoding is used in Galko's scheme. However, it should be pointed out that the standard low pass filter receiver results seem to diverge from Galko's results as the SNR gets larger; this is because Galko calculates a new filter for each SNR. DMSK with receiver 1 and standard filters was also found to outperform DMSK with an MSK type filter as suggested by Aulin et al. [3].

The standard filters will be easier to implement than Galko's optimal linear filters, and will be much easier to implement than a maximum likelihood receiver. The use of standard low pass receivers as the receive filters in and I and Q receiver should thus be considered in the implementation of any of these modulation schemes.

CHAPTER 4

THE EFFECTS OF A NOISY PHASE REFERENCE ON THE PERFORMANCE

The effects of a noisy phase reference on the probability of error were studied for MSK, TFMREC, and DMSK with both receivers. Results are given when the probability density function (pdf) of the phase error is that given when a first order phase locked loop (PLL) is used to recover the carrier reference.

4.1 The Model with a Noisy Phase Reference

The input to the receiver can be written as

$$x(t) = A \cos[\omega_c t + \phi(t) + \theta(t)] + n(t)$$

where $\theta(t)$ is a time varying phase offset. However, in practice $\theta(t)$ varies at a much slower speed than the bit rate. The phase offset can thus be treated as a constant θ. The phase term in the carrier reference, $\hat{\theta}$, is a

random variable whose properties depend on the method used for recovering the carrier. Let $\tilde{\theta} = \theta - \hat{\theta}$. If the expression for the probability of error can be found in terms of $\tilde{\theta}$ then the effect of the noisy phase reference can be found by averaging over all possible $\tilde{\theta}$. The averaging is done as follows:

$$\bar{P}_e = \int_{-\pi}^{\pi} P_e(\tilde{\theta})\, p_{\tilde{\theta}}(\tilde{\theta})\, d\tilde{\theta} \tag{15}$$

where $p_{\tilde{\theta}}(\tilde{\theta})$ is the pdf of $\tilde{\theta}$.

If the pdf of $\tilde{\theta}$ is given by that which occurs when a first order phase locked loop is used for carrier recovery then

$$p_{\tilde{\theta}}(\tilde{\theta}) = \begin{cases} \dfrac{\exp(\mu \cos \tilde{\theta})}{2\pi\, I_o(\mu)} & -\pi < \tilde{\theta} < \pi \\ 0 & \text{elsewhere} \end{cases} \tag{16}$$

where μ is the phase reference signal to noise ratio, and I_o is the modified Bessel function of order zero. Matyas [29] and Rhodes [30] have both used this pdf in their studies on the effects of noisy phase references. This

pdf is plotted for several values of μ in Fig. 4.1.

It is possible to write down the I and Q channel waveforms after the receive filter in terms of $\tilde{\theta}$. The expressions are the same for both of the receivers; the receivers are shown in Figures 2.3 and 2.9. The expressions are:

$$r_I(t) = A \cos[\phi(t) + \tilde{\theta}] * h(t) \tag{17}$$

$$= A\{\cos \tilde{\theta} \cos[\phi(t)] - \sin \tilde{\theta} \sin[\phi(t)]\} * h(t) ,$$

$$r_Q(t) = A \sin[\phi(t) + \tilde{\theta}] * h(t) \tag{18}$$

$$= A\{\sin \tilde{\theta} \cos[\phi(t)] + \cos \tilde{\theta} \sin[\phi(t)]\} * h(t) .$$

4.2 The Performance of the Modulations

The effects of the noisy phase reference can be found by evaluating (12) using (17), or (18), to calculate $r_i(t_k + \gamma)$ for each of the possible waveforms. The result is then substituted into (15) and the integration performed numerically. Simpson's rule was used for the integration in this study. Since the deBuda receiver can resolve a 180° phase ambiguity, the pdf of the phase error should be

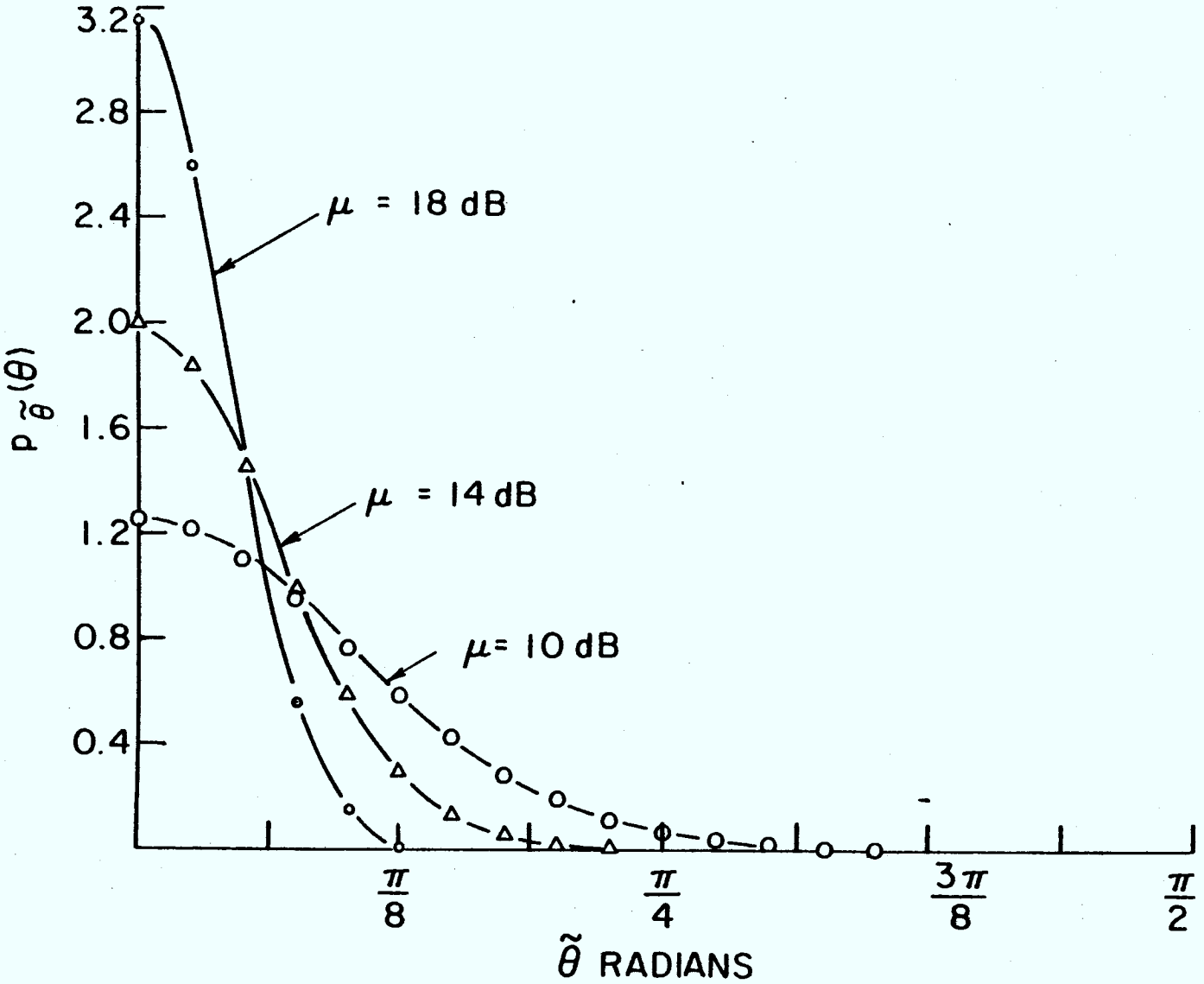

Figure 4.1 : The Probability Density Function for the Phase Error Resulting from a First Order PLL

recalculated as

$$p_{\tilde{\theta}}(\tilde{\theta}) = \begin{cases} \dfrac{\exp(\mu \cos \tilde{\theta})}{2\pi\, I_o(\mu)} + \dfrac{\exp[\mu \cos(\pi - \tilde{\theta})]}{2\pi\, I_o(\mu)} & |\tilde{\theta}| < \dfrac{\pi}{2} \\ 0 & \text{elsewhere} \end{cases}$$

However, as $p_{\tilde{\theta}}(\tilde{\theta})$ in (16) is almost zero for $|\tilde{\theta}| > \pi/4$ this need not be done.

The effects of the noisy phase reference on the probability of error for the modulations is plotted in Figures 4.2 to 4.5; the I and Q receivers with the best standard low pass filter are used for each modulation. It can be seen from the figures that MSK is much less sensitive to a noisy phase reference than the other modulations. In fact, the sensitivity of MSK with the standard low pass filter is almost the same as that found by Matyas [29] when a matched filter was used as the receive filter. The performance losses for the modulations at μ = 18 dB and $P_e = 10^{-4}$ are: 0.6 dB for MSK, 4.8 dB for TFMREC, 2.6 dB for DMSK with receiver 1, and 4.3 dB for

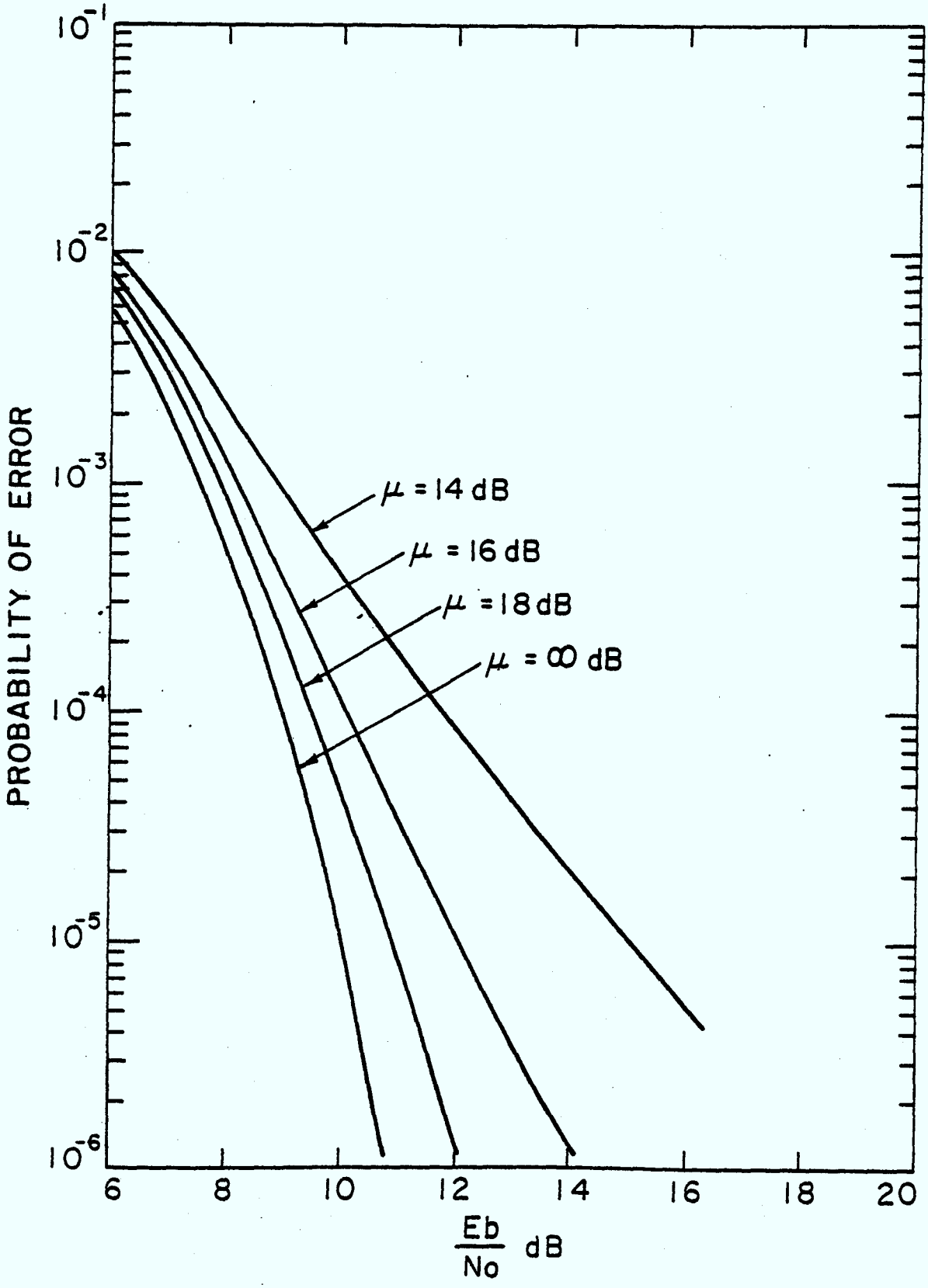

Figure 4.2 : The Effects of a Noisy Phase Reference on the Performance of MSK The Filter is a 2nd Order Butterworth with BT = 0.55

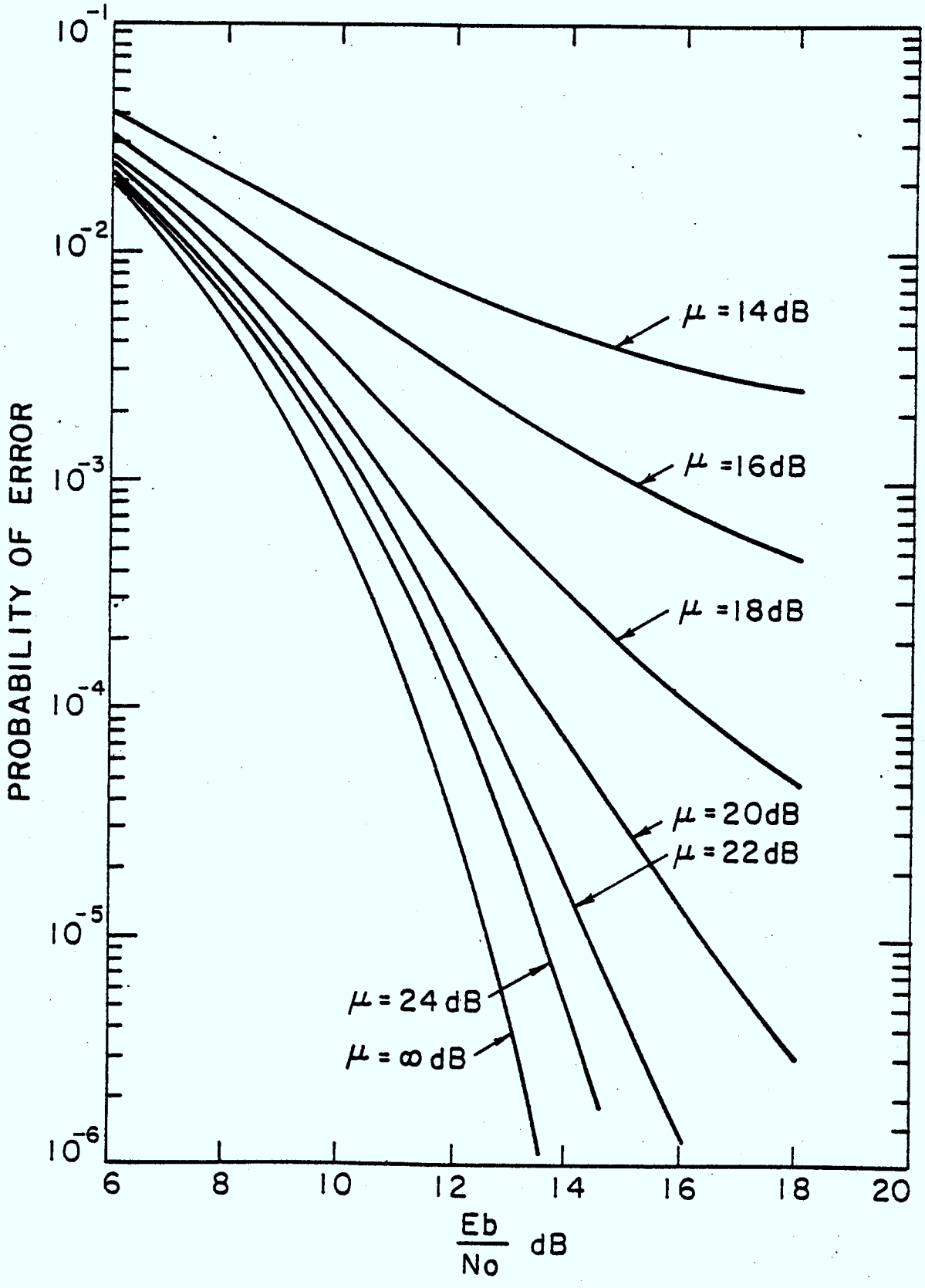

Figure 4.3 : The Effects of a Noisy Phase Reference on the Performance of TFMREC The Filter is a 4th Order Butterworth with BT = 0.6

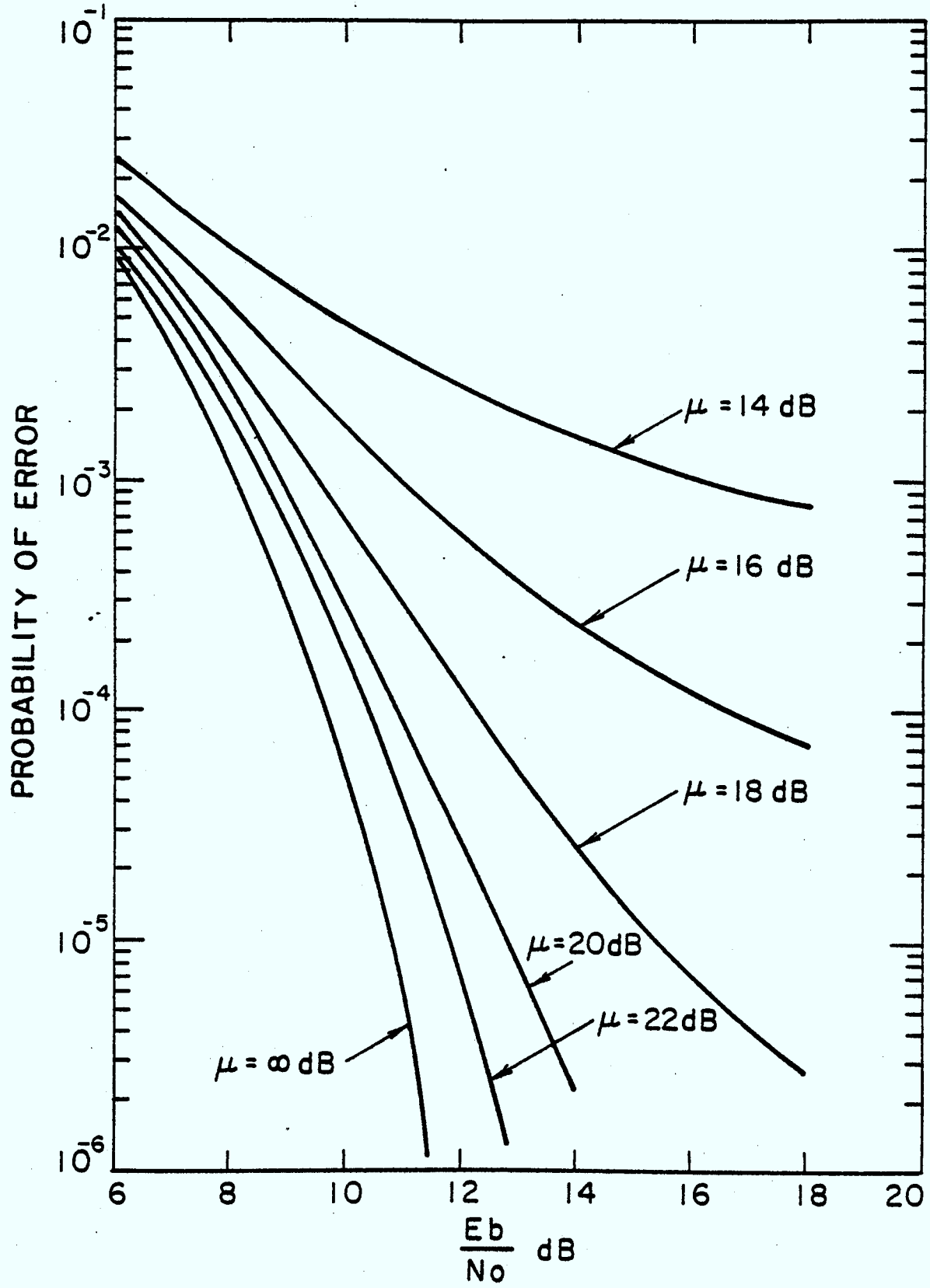

Figure 4.4 : The Effects of a Noisy Phase Reference on the Performance of DMSK with Receiver 1. The Filter is a 4th Order Butterworth with BT = 0.55

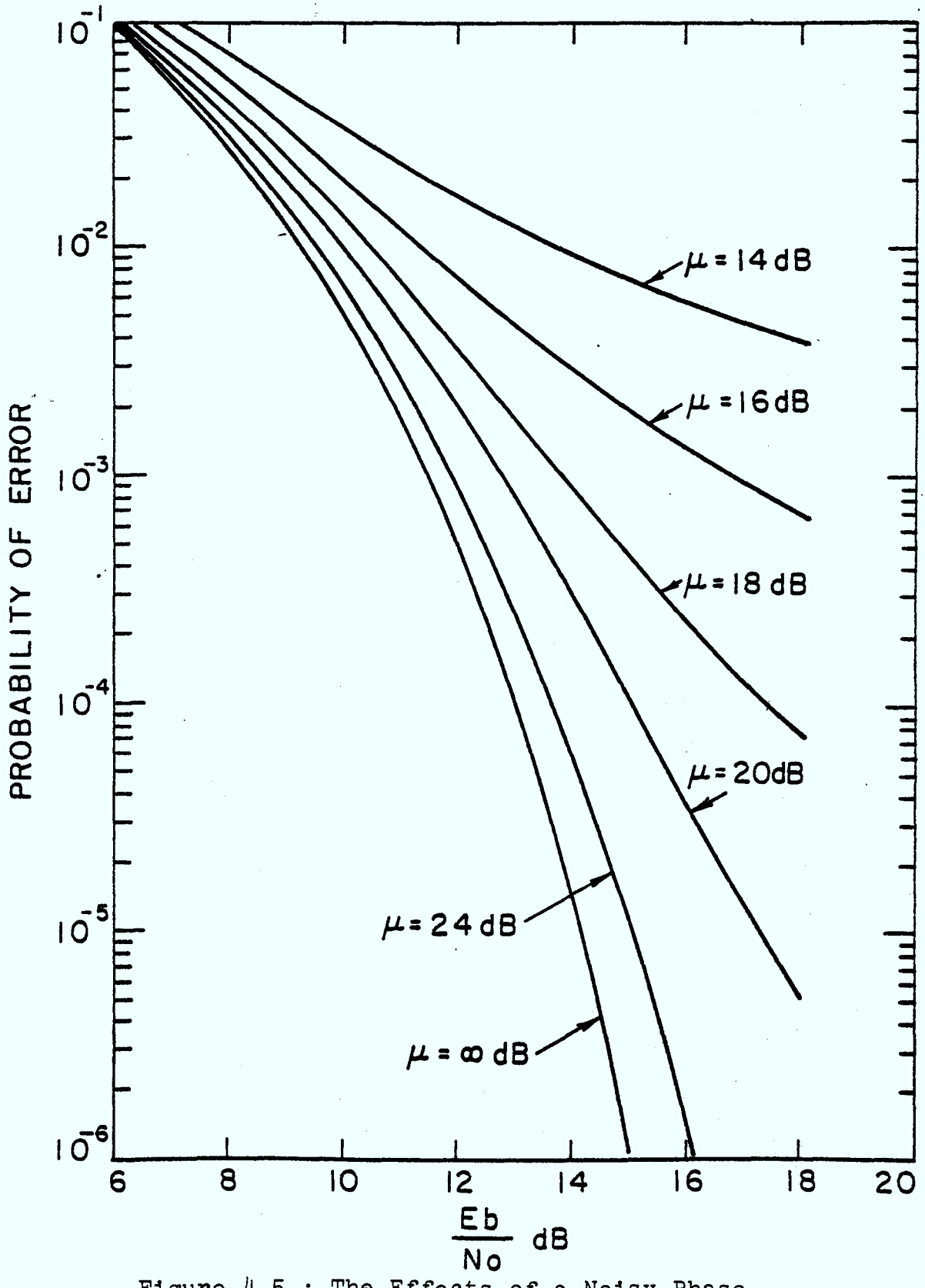

Figure 4.5 : The Effects of a Noisy Phase Reference on the Performance of DMSK with Receiver 2. The Filter is a 4th Order Butterworth with BT = 0.8

DMSK with receiver 2. The amount of loss that is acceptable depends on the design constraints.

The relative sensitivities of the modulations to a noisy phase reference can be explained by considering the $\sin \tilde{\theta} \sin[\phi(t)]$ term in (17); this is interference in the I channel from the Q channel. In MSK this term is always zero at $t = 2kT$ as $\phi(2kT) \in \{0,\pi\}$. The term $\sin \tilde{\theta} \sin[\phi(t)] * h(t)$ will thus still be much smaller than $\cos \tilde{\theta} \cos[\phi(t)] * h(t)$ at $t = 2kT + \gamma$ for any of the $\tilde{\theta}$ where $p_{\tilde{\theta}}(\tilde{\theta})$ is significant. For the other modulations $\sin[\phi(2kT)]$ is often equal to $\cos[\phi(2kT)]$ making the term $\sin \tilde{\theta} \sin[\phi(t)] * h(t)$ at $t = 2kT + \gamma$ large enough to have an important effect on the sample $r_i(2kT + \gamma)$. This increased interference causes the increased sensitivity to a noisy phase reference for TFMREC and DMSK.

Receiver 2 for DMSK can resolve a 90° phase ambiguity, and thus better carrier recovery techniques should be available for this receiver. Better recovery will result in a higher phase reference signal to noise ratio than in the other modulations.

CHAPTER 5

THE EFFECTS OF TIMING ERRORS ON THE PERFORMANCE

The effects of timing errors on the performance are first found for the case where the receive filter is assumed not to distort the channel waveforms. These results give an intuitive feel for the effects of the timing errors. Numerical results are then given when the distortion of the standard low pass receive filters are included. The effects of timing offsets will be the same in both the I and the Q channels.

5.1 The Performance of MSK Assuming No Filter Distortion

In MSK the phase transitions are always linear with slope $\pm \pi/2T$. Thus, as seen before, the I and Q channel waveforms are composed of half sine pulses of length 2T. By examining the phase tree for MSK, Fig. 2.2, it is seen that

$$r_I(t) = A[a_{2k-1} \cos(\frac{\pi}{2T}t)] + n_i'(t) \qquad (2k-1)T \leq t \leq (2k+1)T$$

$$r_Q(t) = A[a_{2k} \sin(\frac{\pi}{2T}t)] + n_2'(t) \qquad 2kT \leq t \leq (2k+2)T \quad .$$

Therefore, using only the in phase channel sampled at time $t = 2kT + \Delta$ and assuming $|\Delta| \leq T$,

$$P_e(\Delta) = 2\{\frac{1}{2} P_r[A \cos(\frac{\pi}{2T} \Delta) + n_1'(t) < 0 \mid a_{2k-1} = 1]$$

$$+ \frac{1}{2} P_r[A \cos(\frac{\pi}{2T} \Delta) + n_2' \geq 0 \mid a_{2k-1} = -1]\}$$

$$= 2 P_r[n_1(t) \geq A \cos(\frac{\pi}{2T} \Delta)]$$

$$= 2 Q\left[\frac{A}{\sigma_{n'}} \cos(\frac{\pi}{2T} \Delta)\right] \quad . \qquad (19)$$

The factor of two is due to the error run property of the deBuda receiver. The probability of error in (19) is plotted against $A^2/\sigma^2_{n'}$ in Fig. 5.1 for various values of Δ .

5.2 The Performance of TFMREC Assuming No Filter Distortion

The possible I and Q channel waveforms over two bit intervals for all possible initial states are shown

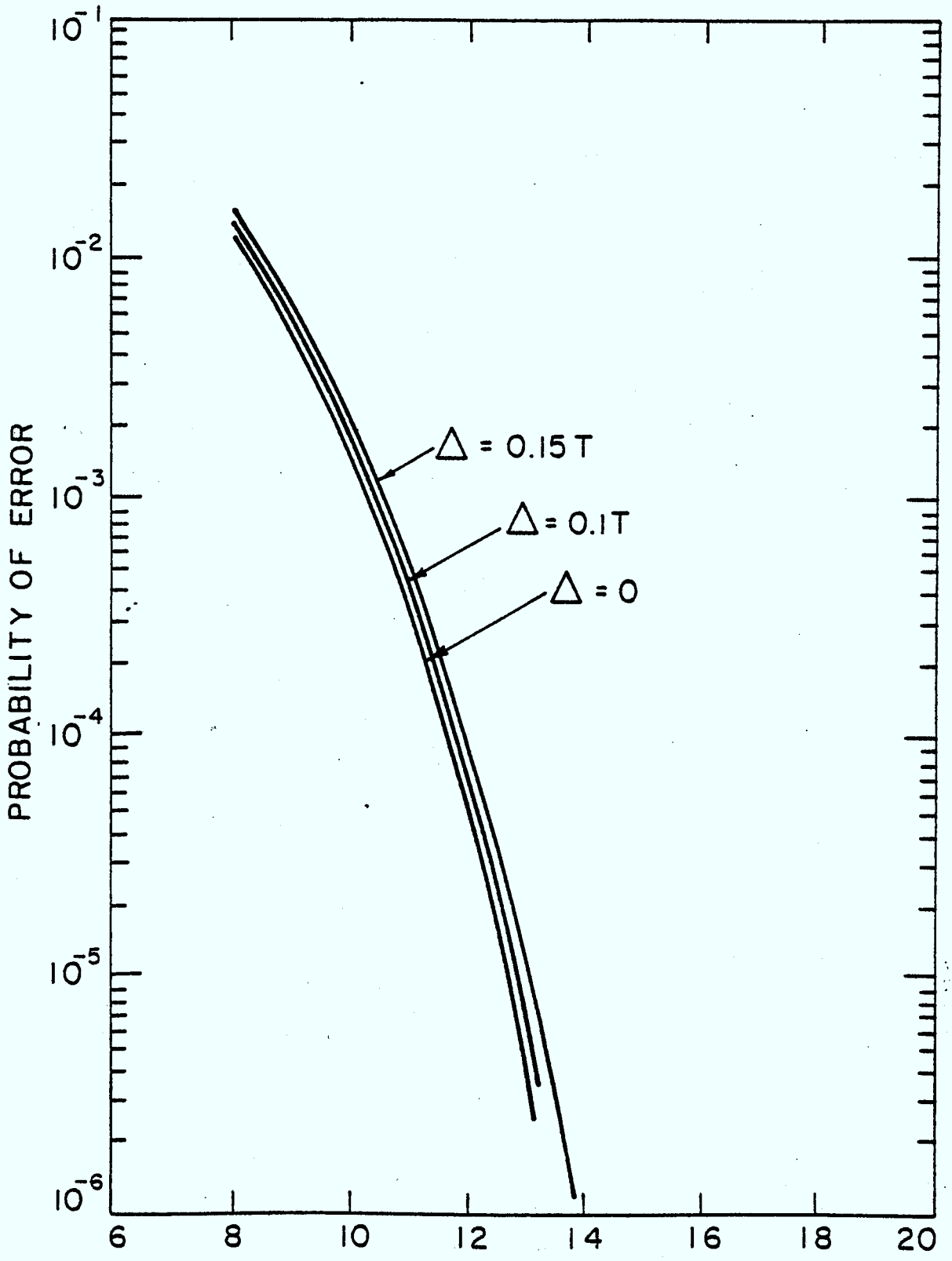

Figure 5.1 : The Timing Error Sensitivity for MSK Assuming No Filter Distortion

in Fig. 3.3 for TFMREC. Each of the four sub-figures contain the waveforms for the four possible combinations of bits, each of which is equiprobable. Due to the symmetry of the waveforms it is necessary to consider only cases 3.3(b) and 3.3(c) in the computation of the error probability; the other two cases will yield duplicate results.

The effect of the timing errors is independent of the sign of Δ . Therefore, considering only negative Δ and $|\Delta| \leq T$,

$$P_e(\Delta) = 2\{\tfrac{1}{4} P_r\{A \sin[\tfrac{\pi}{2T}(T + \Delta) + n_1'(t)] \leq 0\}$$

$$+ \tfrac{1}{4} P_r\{A \sin[\tfrac{\pi}{4T}(T - |\Delta|) + n_1'(t) \leq 0\}$$

$$+ \tfrac{1}{4} P_r\{A \sin[\tfrac{\pi}{4T}(T - |\Delta|) + \tfrac{\pi}{4}] + n_1'(t) \leq 0\}$$

$$+ \tfrac{1}{4} P_r\{\frac{A}{\sqrt{2}} + n_1'(t) \leq 0\}$$

$$= \tfrac{1}{2} Q(\frac{A}{\sqrt{2}\sigma_{n'}}) + \tfrac{1}{2} Q\{\frac{A}{\sigma_{n'}} \sin[\tfrac{\pi}{2T}(T + \Delta)]\}$$

$$= \tfrac{1}{2} Q\{\frac{A}{\sigma_{n'}} \sin[\tfrac{\pi}{4}(T - |\Delta|)]\} + \tfrac{1}{2} Q\{\frac{A}{\sigma_{n'}} \sin[\tfrac{\pi}{4}(T - |\Delta|) + \tfrac{\pi}{4}]\}. \quad (20)$$

The additional factor of two is due to the error run property of the receiver.

The probability of error in (20) is plotted against A^2/σ_n^2, in Fig. 5.2 for various values of Δ. It is seen that TFMREC is more sensitive to timing errors than is MSK. This greater sensitivity is due to the

$$A \sin[\tfrac{\pi}{4T}(T - |\Delta|)]$$

term in (20). With zero timing offset this term has a phase of $\pi/4$ radians. The slope of sin(x) at this phase is considerably greater than the slope when the phase is $\pi/2$ radians; the phase of the sinusoid in (19) is $\pi/2$ radians with zero timing offset. The increased slope causes the degradation in performance due to timing errors to increase as the minimum possible sample amplitude decreases faster.

5.3 The Performance of DMSK Assuming No Filter Distortion

The effects of timing errors in DMSK are found in the same way as in the MSK and TFMREC cases. However, in DMSK both of the receivers must be considered separately. The in phase channel waveforms over two bit intervals are shown in Fig. 3.4 for DMSK; they are shown for each of the eight

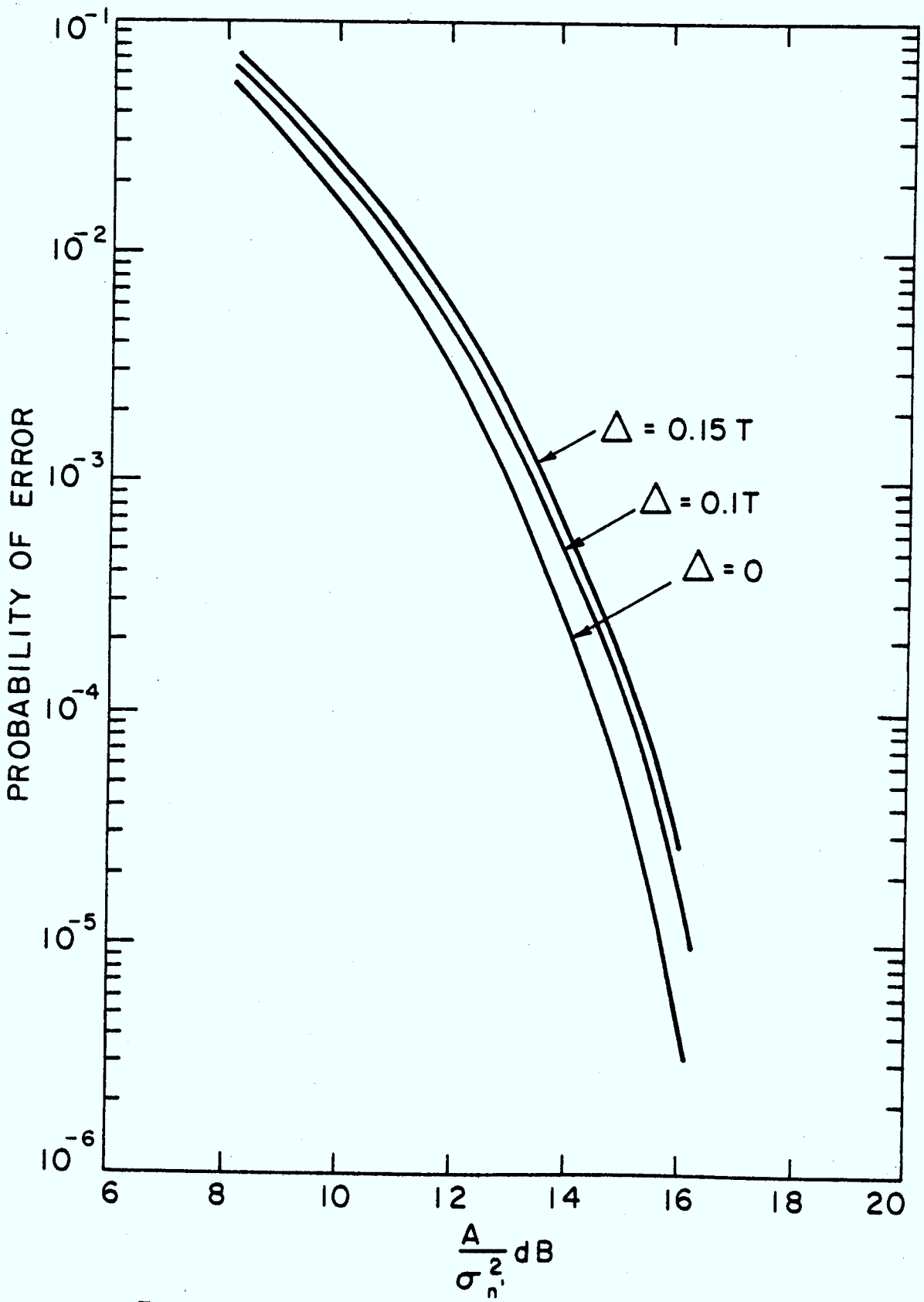

Figure 5.2 : The Timing Error Senstivity for TFMREC Assuming No Filter Distortion

initial states.

When using receiver 1 only Figures 3.4(b) and 3.4(c) are applicable; the other two sub-figures have states that are not allowed for this receiver. The sampling time for the in phase channel is at $t = (2k+1/2)T$. If the offset due to timing errors is restricted such that $|\Delta| \leq T/2$ then,

$$P_e(\Delta) = 2\{\frac{1}{2} P_r[A \cos(\frac{\pi}{2T}\Delta) + n_1'(t) \leq 0]$$

$$+ \frac{1}{2} P_r[\frac{A}{\sqrt{2}} + n_1'(t) \leq 0]\}$$

$$= Q(\frac{A}{\sqrt{2}\ \sigma_{n'}}) + Q\left[\frac{A}{\sigma_{n'}} \cos(\frac{\pi}{2T}\Delta)\right] \quad . \qquad (21)$$

The factor of two is due to the error run property of the receiver.

When using receiver 2, symmetry allows us to consider only Figures 3.4(a) and 3.4(b). With receiver 2 a factor of four is found in front of the expression for the probability of error; a factor of 2 for the error run property, and a factor of 2 because an error in either channel will cause a phase error. The errors in the two

channels are assumed to be independent. The error probability is the same for both positive and negative Δ . Thus, assuming that Δ is negative, $|\Delta| \leq T/2$, and that the sampling time without an offset is 2kT,

$$P_e(\Delta) = 4\{\tfrac{1}{2} P_r[\frac{A}{\sqrt{2}} + n_1'(t) \leq 0]$$

$$+ \tfrac{1}{4} P_r\{A \sin[\tfrac{\pi}{2T}(T - |\Delta|) + \tfrac{\pi}{4}] + n_1'(t) \leq 0\}$$

$$+ \tfrac{1}{4} P_r\{A \cos[\tfrac{\pi}{2T}(T - |\Delta|) + \tfrac{\pi}{4}] + n_1'(t) \geq 0\}$$

$$= 2Q(\frac{A}{\sqrt{2}\,\sigma_{n'}}) + Q\{\frac{A}{\sigma_{n'}} \sin[\tfrac{\pi}{2T}(T - \Delta) + \tfrac{\pi}{4}]\}$$

$$+ Q\{\frac{A}{\sigma_{n'}} |\cos[\tfrac{\pi}{2T}(T - |\Delta|) + \tfrac{\pi}{4}]|\} \quad . \qquad (22)$$

The expressions for the probability of error in (21) and (23) are plotted against $A^2/\sigma_{n'}^2$ in Fig. 5.3 for various values of Δ . It is seen that DMSK with receiver 2 has the greatest, and DMSK with receiver 1 the least sensitivity to timing errors when compared with MSK and TFMREC. DMSK with receiver 1 has the least sensitivity as half of the

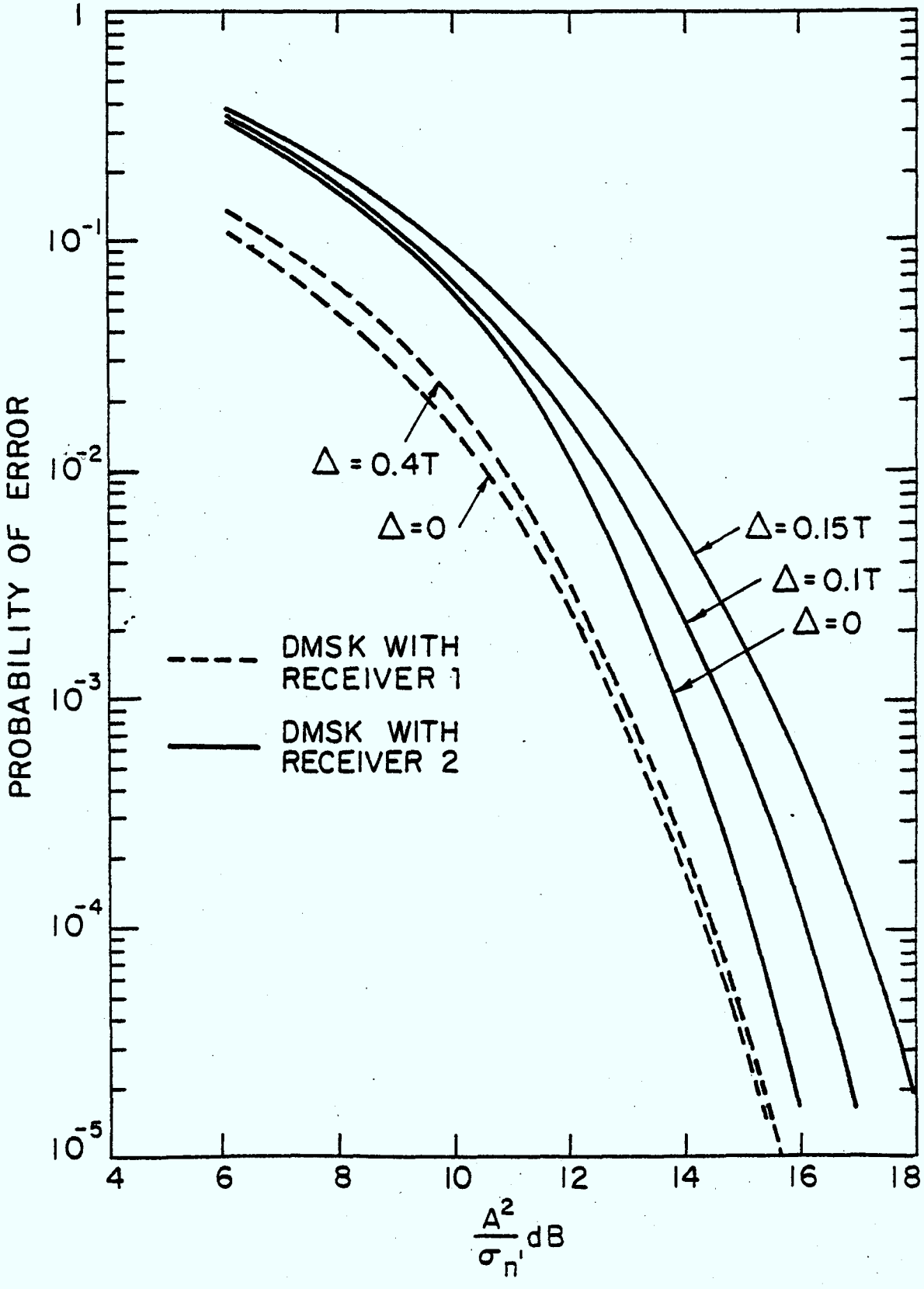

Figure 5.3 : The Timing Error Sensitivity For DMSK Assuming No Filter Distortion

time the timing offset has no effect on the sample magnitude, while the rest of the time the effect is the same as with MSK. Also, in (21) the dominant term in the expression is the one that is independent of the timing offsets. DMSK with receiver 2 is worse than TFMREC as the critical terms in (22) are sinusoids that have a phase of $\pi/4$ radians when sampled with no timing offset but have twice the frequency of the critical term in (20). The higher frequency causes the slope to increase, resulting in the increased sensitivity.

In summary, assuming no filter distortion the modulations can be ranked in order of increasing sensitivity to timing errors as follows: DMSK with receiver 1, MSK, TFMREC, DMSK with receiver 2.

5.4 The Performance of the Modulations Including Filter Distortion

The performance of the modulations with timing offsets was found by replacing Υ by $\Upsilon + \Delta$ in (12). The calculations were made using the I and Q receivers with the best standard low pass filters as the receiver filters. The probability of error is plotted against the signal to noise ratio for various values of Δ in Figures 5.4 to

5.6 for MSK, TFMREC and DMSK respectively. The sampling offset, γ , constant in this analysis, and is the same as the offset calculated in Chapter 3. The timing offset Δ is used to perburb this value. The same analysis technique is used as in Chapter 3.

In general the sensitivity to timing errors is found to be slightly larger for each of the modulations when filter distortion is included; the exception is MSK where it is slightly less. Also, when distortion effects are included MSK becomes the modulation with the least sensitivity the new ranking for timing error sensitivity becomes: MSK, DMSK with receiver 1, TFMREC, DMSK with receiver 2.

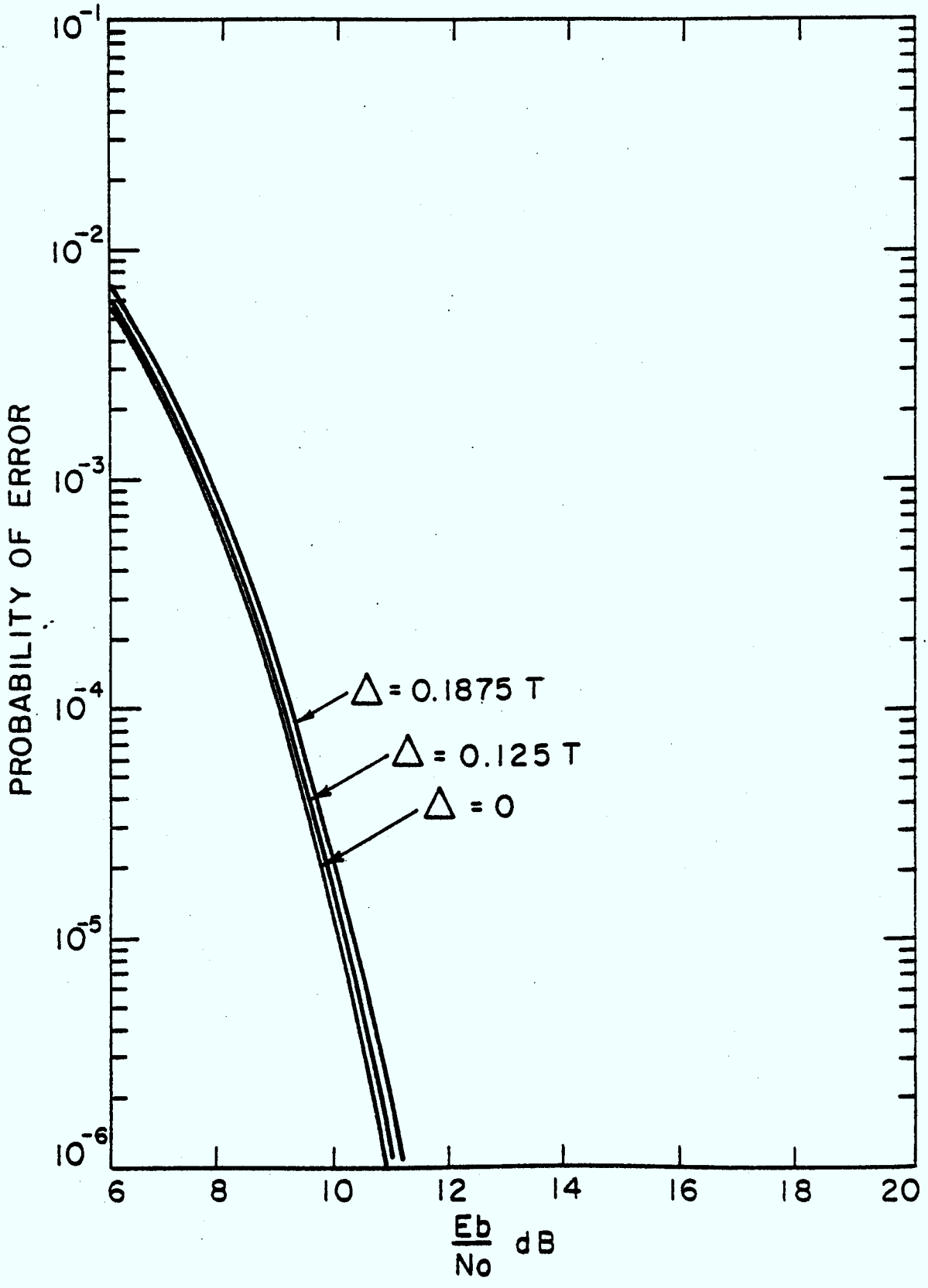

Figure 5.4 : The Sensitivity of MSK to Timing Errors
The Filter is a 2nd Order Butterworth
With BT = 0.55

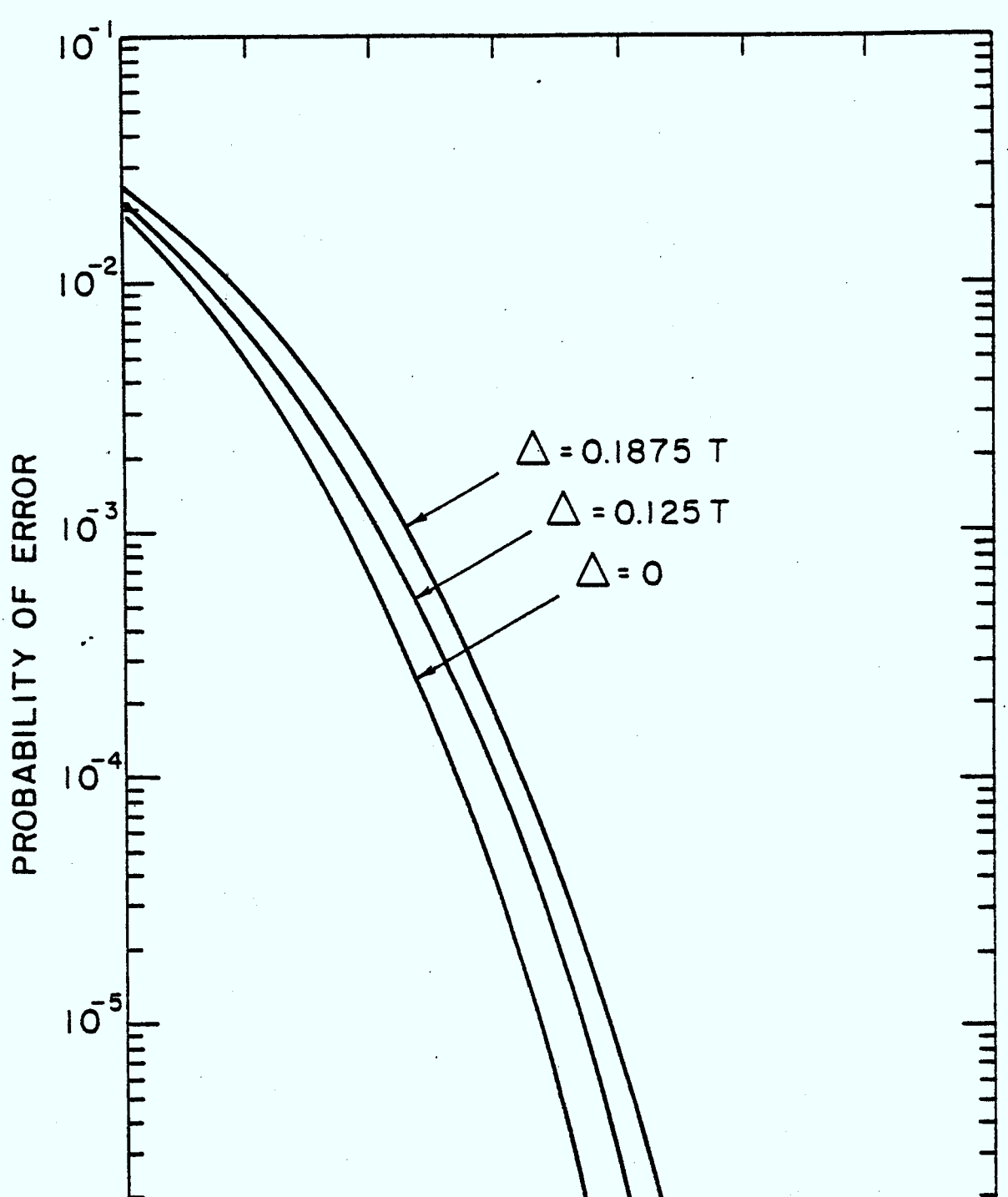

Figure 5.5 : The Sensitivity of TFMREC to Timing Errors
The Filter is a 4th Order Butterworth with
BT = 0.6

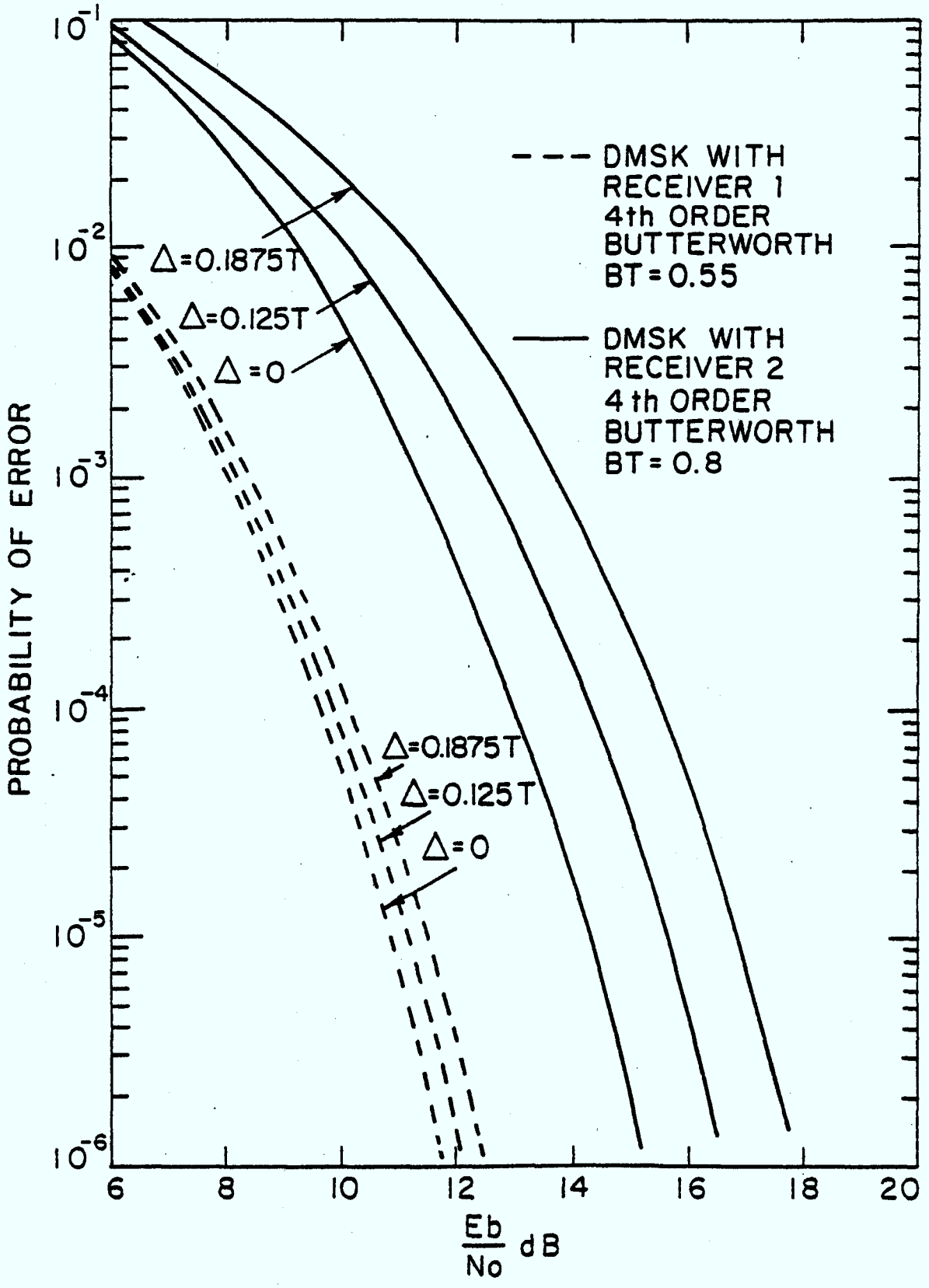

Figure 5.5 : The Sensitivity of DMSK to Timing Errors

CHAPTER 6

CONCLUSION

6.1 Summary

The use of bandwidth-efficient modulations in digital data communications is an important area of research. In this report the use of standard low pass filters as the receive filters in suboptimal, I and Q , receivers for MSK, TFMREC, and DMSK is considered. Each of these modulations is from the class of continuous phase modulations with modulation index h = 1/2.

The system model and the general expression for continuous phase modulations is discussed in Chapter 1. The specific modulations and the receivers for each are presented in Chapter 2.

A numerical method for calculating the performance of each of the modulations with arbitrary filters as the arm filters for the receivers is given in Chapter 2. The method assumes that: the additive noise is white Gaussian noise, there is no signal distortion over the channel, and

that the samples of the noise component at the receive filter output are uncorrelated from sample to sample. The use of Butterworth and Chebychev low pass filters as the receive filters is then considered. The filter from this class that gives the lowest probability of error is then found for each modulation. This probability of error is then compared to the error probabilities obtained with other, more complicated, receive filters.

The effects on the performance of a noisy phase reference and timing errors are examined in Chapters 4 and 5. In these investigations the I and Q receiver uses the best filter of Chapter 3 as the receive filter for each modulation.

6.2 Conclusions

A receiver has been developed for DMSK that can resolve a 90° phase ambiguity in the phase reference. However, this receiver performs more than 3 dB worse than DMSK with a deBuda type receiver, and is more sensitive to a noisy phase reference and timing errors. Thus, this receiver should not be used unless the property of being able to resolve the 90° ambiguity is of overriding concern.

It was found that standard low pass filters can be used quite effectively as the receive filters of the sub-optimal, I and Q , receivers used in this thesis. The best low pass filters for the modulations were: a second order Butterworth filter with BT = 0.55 for MSK; fourth order Butterworth filters for TFMREC, DMSK with receiver 1, and DMSK with receiver 2 where BT = 0.6, 0.55, and 0.8 respectively. For MSK, the best low pass filter resulted in a receiver whose performance was only 0.5 dB away from that of the matched filter receiver. For TFMREC and DMSK, the performance was only 1.6 dB and 0.7 dB worse than the performance of Galko's receivers [17] with his optimal linear filters. Differential encoding was used in the schemes in this thesis, while it is not used in the matched filter receiver, or Galko's receivers. The standard low pass filters are much simpler than the matched filters and Galko's filters, and will be a better design choice in many design situations.

MSK was found to have both the best probability of error, and the least sensitivity to a noisy phase reference and timing errors. However, MSK has fairly poor bandwidth efficiency and is thus unsuitable in some situations. DMSK was found to have better probability of error than

TFMREC, as it also does when maximum likelihood receivers are used. DMSK also has significantly less sensitivity to a noisy phase reference and slightly less sensitivity to timing errors than does TFMREC. Thus, in a system using simple receivers which requires only the out-of-band rejection of DMSK, and not that of TFMREC, DMSK should be used in preference to TFMREC.

6.3 Suggestions for Further Work

A few possible extensions to the work in this report are given below.

1. The performance of suboptimal, I and Q , receivers with standard low pass filters as the receive filters should be studied for more modulations, such as TFM, where g(t) is not rectangular.

2. The receivers discussed in this thesis should be built and experimental results compared to theoretical ones.

3. The possibility of using analytical techniques to find the best standard low pass filter should be considered; the method of Galko and

Pasupathay [23] for the design of optimal linear filters could provide a starting point.

4. Special carrier recovery techniques should be examined for the different CPM schemes.

5. The performance degradation when non-linear and bandlimited channels are used should be compared between the receivers in this report and other more complicated ones. Also, does the best standard low pass filter change with the channel type? Some channels of interest are those which are bandlimited to a high enough degree to cause a significant amount of intersymbol interference.

REFERENCES

[1] Baker, T.J., "Asymtotic Behavior of Digital FM Spectra," IEEE Transactions on Communications, vol. COM-22, pp. 1585-1594, Oct. 1974.

[2] Aulin, T., "Viterbi Detection of Continuous Phase Modulated Signals," National Telecommunications Conference Record, Houston, Dec. 1980, pp. 14.2.1 - 14.2.7.

[3] Aulin, T., Sundberg, C.E., and Svensson, A., "Modified Offset Quadrature Receivers for Partial Response Continuous Phase Modulation," Technical Report TR-152, June 1981, Telecommunication Theory, University of Lund, Sweden.

[4] Osborne, W.P., and Luntz, M.B., "Coherent and Non-Coherent Detection of CPFSK," IEEE Transactions on Communications, vol. COM-22, pp. 1023-1036, Aug. 1974.

[5] deJager, F., and Dekker, C.E., "Tamed Frequency Modulation, a Novel Method to Achieve Spectral Economy in Digital Transmission," IEEE Transactions on Communications, vol. COM-26, No. 5, pp. 534-542, May 1978.

[6] Jones, J.J., "Filter Distortion and Intersymbol Interference Effects on PSK Signals," IEEE Transactions on Communication Technology, vol. COM-19, No. 2, pp. 120-132, April 1971.

[7] Lender, A., "The Duobinary Technique for High Speed Data Transmission," IEEE Transactions on Communications Electronics, pp. 214-218, May 1963.

[8] deBuda, R., "Coherent Demodulation of Frequency Shift Keying with Low Deviation Ratio," IEEE Transactions on Communications, vol. COM-20, pp. 429-435, June 1972.

[9] Kabal, P., and Pasupathay, S., "Partial Response Signaling," IEEE Transactions on Communications, vol. COM-23, No. 9, Sept. 1975.

[10] Haykin, S., Communication Systems, New York : J. Wiley and Sons, 1978.

[11] Anderson, J.B., Sundberg, C.E., Aulin, T., and Rydbeck, N., "Power Bandwidth Performance of Smooth Phase Modulation Codes," IEEE Transactions on Communications, vol. COM-29, No. 3, pp. 187-195, March 1981.

[12] Aulin, T., and Sundberg, C.E., "Continuous Phase Modulation – Part I : Full Response Signaling," IEEE Transactions on Communications, vol. COM-29, No. 3, pp. 196-209, March 1981.

[13] Aulin, T., Rydbeck, N., and Sundberg, C.E., "Continuous Phase Modulation – Part II : Partial Response Signaling," IEEE Transactions on Communications, vol. COM-29, No. 3, pp. 210-225, March 1981.

[14] Deshpande, G.S. and Wittke, P.H., "Correlative Encoded Digital FM," IEEE Transactions on Communications, vol. COM-29, No. 2, pp. 156-162, Feb. 1981.

[15] Aulin, T., Lindall, G., and Sundberg, C.E., "Partial Response CPM Schemes With Short Pulses – Tradeoff Between Error Probability and Spectrum," Technical Report TR-140, May 1980, Telecommunication Theory, University of Lund, Sweden.

[16] Deshpande, G.S., and Wittke, P.H., "Optimum Pulse Shaping in Digital Angle Modulation," IEEE Transactions on Communications, vol. COM-29, No. 2, pp. 162-168, Feb. 1981.

[17] Galko, P., and Pasupathay, S., "Linear Receivers for Generalized MSK," Communications Technical Report, Nov. 1981, Department of Electrical Engineering, University of Toronto.

[18] Pasupathay, S., "Minimum Shift Keying: A Spectrally Efficient Modulation," IEEE Communications Magazine, vol. 17, No. 4, July, 1979.

[19] Gronemeyer, S.A., and McBride, A.L., "MSK and Offset QPSK Modulation," IEEE Transactions on Communications, vol. COM-24, pp. 809-820, Aug. 1976.

[20] Prabhu, V.K., "MSK and Offset QPSK Modulation with Bandlimiting Filters," IEEE Transactions on Aerospace and Electronic Systems, vol. AES-17, No. 1, pp. 2-8, Jan. 1981.

[21] Rhodes, S.A., "FSOQ, A New Modulation Technique That Yields a Constant Envelope," National Telecommunications Conference Record, Houston, Dec. 1980, pp. 51.1.1-51.1.7.

[22] McCreath, D.R., and McLane, P.J., "Filter Parameter Optimization For Linear and Non-Linear BPSK Transmission," IEEE Transactions on Communications, vol. COM-27, No. 1, pp. 191-197, Jan. 1979.

[23] Galko, P. and Pasupathay, S., "Optimal Linear Receiver Filters For Digital Signals," Communications Technical Report, Nov. 1981, Department of Electrical Engineering, University of Toronto.

[24] Galko, P. and Pasupathay, S., "On a Class of Generalized MSK," International Conference on Communications Conference Record, Denver, 1981, pp. 2.4.1-2.4.5.

[25] Wozencraft, J.M., and Jacobs, I.M., Principles of Communications Engineering, New York : J. Wiley and Sons, 1965.

[26] Glave, P.E., "On Upper Bound on the Probability of Error Due to Intersymbol Interference," IEEE Transactions on Information Theory, vol. IT-18, No. 3, May 1972.

[27] Johnson, D.E., Introduction to Filter Theory, Englewood Cliffs: Prentice Hall, Inc., 1976.

[28] Oppenheim, A.V., and Schafer, R.W., Digital Signal Processing, Englewood Cliffs: Prentice Hall, Inc., 1975.

[29] Matyas, R., "Effect of Noisy Phase References on Coherent Detection of FFSK Signals," IEEE Transactions on Communications, vol. COM-26, pp. 807-815, June 1978.

[30] Rhodes, S.A., "Effect of a Noisy Phase Reference on Coherent Detection of Offset-QPSK Signals," IEEE Transactions on Communications, vol. COM-22, pp. 1046-1055, Aug. 1974.

VAISEY, D.J.
Realizable arm filters in I and Q receivers for MSK-type continuous phase modulations